Acta Pharmaceutica Sinica B 2021;11(7):1867−1884

Chinese Pharmaceutical Association
Institute of Materia Medica, Chinese Academy of Medical Sciences

Acta Pharmaceutica Sinica B

www.elsevier.com/locate/apsb
www.sciencedirect.com

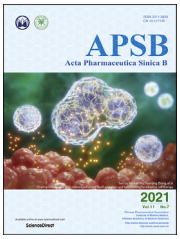

ORIGINAL ARTICLE

A novel PGAM5 inhibitor LFHP-1c protects blood−brain barrier integrity in ischemic stroke

Chenglong Gao[a,†] Yazhou Xu[a,†] Zhuangzhuang Liang[a,†] Yunjie Wang[a], Qinghong Shang[b], Shengbin Zhang[c], Cunfang Wang[c], Mingmin Ni[c], Dalei Wu[b], Zhangjian Huang[a,*] Tao Pang[a,d,*]

[a]*State Key Laboratory of Natural Medicines, Jiangsu Key Laboratory of Drug Screening, Jiangsu Key Laboratory of Drug Discovery for Metabolic Diseases, China Pharmaceutical University, Nanjing 210009, China*
[b]*Helmholtz International Lab, State Key Laboratory of Microbial Technology, Shandong University, Qingdao 266237, China*
[c]*Guangdong Long Fu Pharmaceutical Co., Ltd., Zhongshan 528451, China*
[d]*Key Laboratory of Drug Quality Control and Pharmacovigilance (China Pharmaceutical University), Ministry of Education, Nanjing 210009, China*

Received 23 August 2020; received in revised form 15 October 2020; accepted 16 November 2020

KEY WORDS

Ischemic stroke;
Blood−brain barrier;
Brain microvascular endothelial cells;
Target identification;
Surface plasmon resonance;
PGAM5;
NRF2;
LFHP-1c

Abstract Blood−brain barrier (BBB) damage after ischemia significantly influences stroke outcome. Compound LFHP-1c was previously discovered with neuroprotective role in stroke model, but its mechanism of action on protection of BBB disruption after stroke remains unknown. Here, we show that LFHP-1c, as a direct PGAM5 inhibitor, prevented BBB disruption after transient middle cerebral artery occlusion (tMCAO) in rats. Mechanistically, LFHP-1c binding with endothelial PGAM5 not only inhibited the PGAM5 phosphatase activity, but also reduced the interaction of PGAM5 with NRF2, which facilitated nuclear translocation of NRF2 to prevent BBB disruption from ischemia. Furthermore, LFHP-1c administration by targeting PGAM5 shows a trend toward reduced infarct volume, brain edema and neurological deficits in nonhuman primate *Macaca fascicularis* model with tMCAO. Thus, our study identifies compound LFHP-1c as a firstly direct PGAM5 inhibitor showing amelioration of ischemia-induced BBB disruption *in vitro* and *in vivo*, and provides a potentially therapeutics for brain ischemic stroke.

*Corresponding authors. Tel.: +86 25 83271043, fax: +86 25 83271142 (Tao Pang); Tel.: +86 25 83271072, fax: +86 25 83271015 (Zhangjian Huang).
E-mail addresses: tpang@cpu.edu.cn (Tao Pang), zhangjianhuang@cpu.edu.cn (Zhangjian Huang).
†These authors made equal contributions to this work.
Peer review under responsibility of Chinese Pharmaceutical Association and Institute of Materia Medica, Chinese Academy of Medical Sciences.

https://doi.org/10.1016/j.apsb.2021.01.008

1. Introduction

Ischemic stroke is a significant cause of mortality and long-lasting disability worldwide, with limited effective treatment available to date[1]. The blood−brain barrier (BBB) functions as a selective barrier between brain and circulating blood to maintain brain homeostasis[2], which is disrupted in the early stage of cerebral ischemia[3]. As a crucial member of BBB, endothelial cells serve as the first-line of defense against harmful molecules form peripheral blood[4]. Once ischemia occurs, tight junctions between cerebral endothelial cells are degraded by reactive oxygen species, oxidative stress and matrix metalloproteinases (MMPs), thereby damaging endothelial cells[5]. Furthermore, the damaged endothelial cells could produce cell adhesion molecules and pro-inflammatory factors that recruit leukocytes migration into brain[5]. The inflammatory cytokines released by leukocytes further exaggerate BBB disruption and brain damage[4]. Thus, protection of cerebral endothelial cells and maintenance of BBB integrity could be a promising approach for the treatment of ischemic stroke.

Phosphoglycerate mutase family member 5 (PGAM5) is a mitochondrial Ser/Thr phosphatase normally located in the inner mitochondrial membrane (IMM)[6,7] and regulates mitochondria dynamics, mitophagy, cell death and organelle homeostasis. Nevertheless, there are experimental evidences supporting that PGAM5 is located in the outer mitochondrial membrane (OMN)[6], where its phosphatase domain is accessible from the cytosol[8]. As a number of the PGAM histidine phosphatase superfamily, PGAM5 has the conserved PGAM domain[9]. However, unlike other PGAM members, which are reported to phosphotransferase or phosphohydrolase small-molecular metabolites, PGAM5 dephosphorylates protein substrates[10], through targeting phosphorylated serine, threonine, and histidine residues[11,12]. PGAM5 has been reported to regulate mitochondrial homeostasis and cell death through the regulation of mitochondrial dynamic fusion/fission. During mitochondrial dysfunction caused by cell necrotic death or mitophagy, PGAM5 triggers its GTPase activity and promotes mitochondrial dynamic fission through recruiting and dephosphorylating dynamin-related protein 1 (DRP1) at Ser 637 site[13]. PGAM5 can regulate mitophagy by dephosphorylating FUN14 domain containing 1 (FUNDC1)[14], which is independent of E3 ubiquitin ligase RBR E3 ubiquitin protein ligase (PARKIN). PGAM5 also regulates mitophagy through stabilizing PTEN induced kinase 1 (PINK1) by recruiting PARKIN under stress conditions, and then degrades the damaged mitochondria in a PARKIN-dependent manner[13,15]. PGAM5 can also induce mitochondrial biogenesis by activating WNT signaling through being cleaved and released to cytoplasm in a PARKIN-dependent manner[8]. Besides, experimental evidences support that PGAM5 prevents nuclear factor erythroid 2-related factor 2 (NRF2) activation by forming a tertiary complex with Kelch-like ECH-associated protein 1 (KEAP1) and NRF2, followed by inhibiting the nuclear translocation of NRF2 and regulating anti-oxidative response[16−18]. Chen et al.[19] reported that PGAM5 knockdown alleviates neuronal injury after traumatic brain injury (TBI) through DRP1-mediated mitochondrial dysfunction. Hos et al.[17] reported that type I interferon (IFN−I) induces receptor-interacting protein kinase 3 (RIP3)-mediated PGAM5 expression, and then PGAM5 subsequently interacts with NRF2 (presumably through KEAP1), which sequesters NRF2 in the cytosol, thereby repressing the transcription of NRF2-dependent antioxidative genes.

The transcription factor NRF2 is one of the body's major defense mechanisms, driving transcription of >300 anti-oxidant response element (*ARE*)-regulated genes that are involved in many critical cellular processes including redox regulation, proteostasis, xenobiotic detoxification, and primary metabolism, and plays an important role in neurological disorders[17]. It has been reported that activation of NRF2 could reduce the production of reactive oxygen species (ROS) and increase the expressions of anti-oxidant genes, which is associated with protection against ischemic stroke[20].

LFHP-1c, as a small molecular hybrid compound bearing 2-(1-hydroxypentyl)-benzoate (HPBA) and telmisartan moieties (Supporting Information Fig. S1), has been reported in our previous studies to inhibit microglial activation and ameliorate neuroinflammation *via* both 5′-adenosine monophosphate-activated protein kinase (AMPK) and NRF2 activation during ischemic stroke[21]. However, whether LFHP-1c improves BBB integrity through preventing cerebral endothelial cells dysfunction to show beneficial effects on ischemic stroke, as well as the target protein of LFHP-1c, remain unknown. In this study, we demonstrated that LFHP-1c attenuated ischemia-induced brain infarction, brain edema and blood−brain barrier disruption *in vivo*. And *in vitro* BBB model, which was established by co-culture of rat brain microvascular endothelial cells and astrocytes, was taken to study the effect of LFHP-1c against oxygen-glucose deprivation/reoxygenation (OGD/R) injury mimicking *in vivo* ischemia condition. Furthermore, we presented that, for the first time, LFHP-1c directly bound with PGAM5, inhibited both PGAM5 enzyme activity and the interaction between PGAM5 and NRF2, and thereby inducing nuclear translocation of NRF2 in rat brain microvascular endothelial cells (rBMECs) for anti-oxidative genes expression. Thus, LFHP-1c protected rBMECs and BBB integrity against ischemia through PGAM5/NRF2 axis, which have been demonstrated *in vitro* and *in vivo*.

2. Materials and methods

2.1. Materials

DMSO, Evans blue, triphenyltetrazolium chloride (TTC), PLL, DNase I, copper (II) sulfate ($CuSO_4$), Tris (2-carboxyethyl) phosphine (TCEP), DTT and the click chemistry ligand tris [(1-benzyl-1*H*-1,2,3-triazol-4-yl)methyl]amine (TBTA) were purchased from Sigma−Aldrich (St. Louis, MO, USA). Serine/Threonine Phosphatase Assay System (V2460) was purchased from Promega (WI, USA). Biotin-PEG_3-N_3 was purchased from Click Chemistry Tools (AZ104, Scottsdale, AZ, USA). Streptavidin Mag Sepharose™ (Code No. 28-9857-38), MagRack 6 (Code No. 28-9489-64), Ni-NTA resin, and Superose 6 10/300 GL Increase column were purchased from GE Healthcare (Pittsburgh, PA, USA). The QuickBlue staining kit was purchased from Biodragon Immunotechnologies Co., Ltd. (Beijing, China). IPTG was purchased from CSNpharm (Chicago, IL, USA). 3D photo-crosslinking nanosensor chip was purchased from Better-Ways Inc (Guangzhou, China). Chip array printer was purchased from BioDot Corporation (CA, USA). DMEM, DMEM/F-12, trypsin, Alexa Flour™ 488® goat anti-rabbit IgG (H + L), Alexa Flour™ 633® goat anti-mouse IgG (H + L), Novex™ Tris-

Glycine SDS Sample Buffer (2×) and carboxy-H_2DCFDA probes were purchased from Invitrogen (Carlsbad, CA, USA). RIPA Lysis and Extraction Buffer, ethylenediaminetetraacetic acid (EDTA), Pierce Protease and Phosphatase Inhibitor Mini Tablets (EDTA-free), Halt™ Protease Inhibitor Cocktail and Pierce™ BCA Protein Assay Kit were purchased from Thermo Scientific (Waltham, MA, USA). Fetal bovine serum (FBS) was purchased from Clark Bioscience (Shanghai, China). Endothelial cell medium (ECM) was purchased from ScienCell™ Research Laboratories (San Diego, CA, USA). Trizol reagent, the cDNA synthesis kit and SYBR Green were purchased from Vazyme (Nanjing, China). The cytoplasmic and mitochondria extraction kit, the cytoplasmic and nuclear protein extraction kit, LDH assay kit, bovine serum albumin (BSA), PBS, HBSS, HEPES, terminal deoxynucleotidyl transferase-mediated dUTP nick-end labeling (TUNEL) apoptosis assay kit, protein A/G agarose and Hoechst 33342 were purchased from Beyotime Biotechnology (Shanghai, China). Rabbit anti-ZO-1 (1:1000 or 1:250), rabbit anti-occludin (1:1000), rabbit anti-LAMB1 (1:1000) and rabbit anti-HO-1 (1:1000, for rat protein samples) were purchased from Proteintech Group (Rosemont, IL, USA). Rabbit anti-VCAM-1 (1:1000), rabbit anti-PGAM5 (1:1000), rabbit anti-COXIV (1:1000), rabbit anti-β-actin (1:1000), rabbit anti-GAPDH (1:1000), rabbit anti-H3 (1:1000) and mouse anti-α-tubulin (1:1000) were purchased from ABclonal (Wuhan, China). Rabbit anti-HO-1 (1:500, for *Macaca fascicularis* protein samples), rabbit anti-GFAP (1:500) and Alexa Fluor 488® conjugated goat anti-rat IgG were purchased from Abcam (Cambridge, MA, USA). Mouse anti-PGAM5 (1:50) and rabbit anti-NRF2 (1:1000) were purchased from Santa Cruz Biotechnology (CA, USA). Rabbit anti-p-DRP1 at Ser 637 (1:500, for rat protein samples) was purchased from Cell Signal Technology (Beverley, MA, USA). Rabbit anti-p-DRP1 at Ser 637 (1:500, for *M. fascicularis* protein samples) was purchased from Affinity Biosciences (Cincinnati, OH, USA). Mouse anti-CD31 (1:250) was purchased from Merck Millipore (Billerica, MA, USA). HRP goat anti-rabbit IgG (H + L) (1:10,000) and HRP goat anti-mouse IgG (H + L) (1:10,000) were purchased from ABclonal (Wuhan, China). Chemiluminescence detection reagents and polyvinylidene difluoride (PVDF) membranes were purchased from Millipore (Billerica, MA, USA). BASF was purchased from Beijing Fengli Jingqiu Pharmaceutical Co., Ltd. (Beijing, China). Isoflurane and MCAO monofilament nylon suture were purchased from RWD Co., Ltd. (Shenzhen, China). Electronic scale for weighting animals was purchased from Ding Jing Yao (Hangzhou, China) and was calibrated as $d = 0.1$ g. Electronic balance (Sartorius, Göttingen, Germany) for weighting compounds in biological experiments or rat brains in animal experiments were calibrated as $d = 0.01$ mg. Syringes, which specification is one mL were purchased from Jiangsu Great Wall Medical Devices Co., Ltd. (Jiangsu, China). All other chemicals and reagents were of analytical grade.

2.2. Animals

All rat animal experiments were approved by the Administration Committee of Experimental Animals in Jiangsu Province and the Ethics Committee of China Pharmaceutical University and carried out in accordance with Stroke Treatment Academic Industry Roundtable (STAIR) guidelines and the National Institutes of Health (NIH) Guide for the Care and Use of Laboratory Animals.

Three-week-old SD rats and male adult SD rats weighting 230−250 g were purchased from SPF (Beijing) Biotechnology Co., Ltd. (Beijing, China). All animals were housed under standard SPF housing environment at a temperature between 21 and 25 °C with a 12-h light/dark cycle and a relative humidity from 40% to 60%, with ad libitum access to rodent chow and water.

All animal experiments in *M. fascicularis* were performed at Wincon TheraCells Biotechnologies (Nanning, China) accordance with the NIH Guide for the Care and Use of Laboratory animals and according to requirements of the "Laboratory Animal Management" (2nd Edition) promulgated by the Chinese Science and Technology Commission in 1988. All the animal experiment protocols were approved by Wincon TheraCells Biotechnologies Institutional Animal Care and Use Committee (W00151). Fourteen healthy male *M. fascicularis* (7−10 years old, 6−11 kg body weight) obtained from XiongSen Primate Laboratory Animal Breeding Development Company (Yulin, China) were used. Monkeys were housed under standard conditions with temperatures at 20−28 °C and a controlled 12-h light/dark cycle under a humidity of 40%−70%. All monkeys were allowed free access to water and food.

2.3. Transient middle cerebral artery occlusion surgery and drug administration

2.3.1. Transient middle cerebral artery occlusion surgery and drug administration in SD rats

Transient MCAO model was performed as previously reported[21]. Briefly, rats were anesthetized with Isoflurane (RWD Life Science Co., Ltd.), and then the right common carotid artery (CCA), external carotid artery (ECA), and internal carotid artery (ICA) were surgically isolated and exposed. A silicone coated nylon thread was inserted into ICA and advanced to occlude the origin of the middle cerebral artery (MCA). After 2 h occlusion of cerebral blood flow, the filament was gently withdrawn to accomplish reperfusion. The body temperature of rats was maintained at 37.0 °C with a heating pad. And the cerebral blood flow was monitored by laser Doppler flowmetry (Moor Instruments, Millwey, UK).

LFHP-1c was dissolved in the vehicle of 10% DMSO (Sigma−Aldrich), 20% BASF (Beijing Fengli Jingqiu Pharmaceutical Co., Ltd.) plus 70% saline. For determining the therapeutic window of LFHP-1c treatment, the rats were randomly divided into four groups, including Sham, Vehicle, LFHP-1c (4 h) and LFHP-1c (12 h). Rats in LFHP-1c (4 h) and LFHP-1c (12 h) groups were intravenously injected respectively with LFHP-1c (5 mg/kg, 0.5 mL volume) at four or 12 h after ischemia onset, and then injected another time at 24 h post-ischemia. Rats in the Sham and Vehicle group were injected with the vehicle equal to that in LFHP-1c group. To study the dose-dependent effects of LFHP-1c, the rats were randomly assigned to four groups: Sham, Vehicle, and LFHP-1c (1 or 5 mg/kg) groups. Rats in the LFHP-1c-treated groups were intravenously injected with LFHP-1c (1 or 5 mg/kg) at 4 h and again at 24 h after ischemia onset. Rats in the Sham and Vehicle group were injected with the vehicle equal to that in LFHP-1c group.

2.3.2. Transient middle cerebral artery occlusion surgery and drug administration in M. fascicularis

Twelve of 14 *M. fascicularis* were subjected to transient middle cerebral artery occlusion (tMCAO) surgery, and the other two *M. fascicularis* were received sham operation. All monkeys were fasted for 16 h before the surgery. Anesthesia was induced by ketamine (10 mg/kg, IM; Bucolic, Jiangsu, China) and atropine

sulfate (0.04 mg/kg, IM; Henan Runhong Pharmaceutical Co., Ltd., Henan, China), and maintained with Isoflurane (2%−3%, oxygen flow at 0.6 L/min; RWD Life Science Co., Ltd.) *via* intubation. Lactated ringers (5−10 mL/kg/h; Kelun, Hunan, China) and ampicillin sodium injection (1 g per monkey; Shandong Lukang Biological Manufacturing Co., Ltd., Shandong, China) were intravenously administrated during the surgery. The body temperature of monkeys was maintained with heating pad. The physiological parameters including heart rate, blood pressure, respiratory rate, body temperature and blood oxygen saturation were monitored and recorded every 15 min throughout the surgery until the monkeys recovered consciousness.

Transient MCAO model in *M. fascicularis* was performed as previous described[22]. Skin in the upper anterior segment of the left zygoma was cut off to fully expose the skull. The cranial bone was drilled along the upper edge of the sphenoid bone with a craniotomy, and the skull at the front end of the lateral sulcus was removed with the size about 2 cm × 2 cm. The dura was opened to expose M1 segment of the middle cerebral artery. Then proximal M1 segment was fully exposed and clamped with a microvascular aneurysm clip. Saline was utilized to keep the brain surface moist. After 1 h occlusion, the clip was released to accomplish reperfusion. The dura mater was stitched. Then subcutaneous tissue and skin closure were conducted. The monkeys were given tramadol injection (15 lactated ringers 25 mg/day; Shanghai Harvest Pharmaceutical Co., Ltd., Shanghai, China) and ampicillin sodium injection (100 mg/kg/day; Shandong Lukang Biological Manufacturing Co., Ltd.) for 3 days after the surgery.

The monkeys subjected to tMCAO surgery were randomly divided to vehicle group and LFHP-1c group. Monkeys in LFHP-1c group were intravenously injected with LFHP-1c (3 mg/kg, one mL/kg) at 4 h, 1, 2 3, 4, 5, 6 and 7 days after tMCAO onset. LFHP-1c was dissolved in the vehicle of 6.67% DMSO (Sigma−Aldrich), 16.67% BASF (Beijing Fengli Jingqiu Pharmaceutical Co., Ltd.) plus 76.66% saline. Monkeys in Sham group and Vehicle group were intravenously administrated with vehicle at the same time points.

2.4. Assessment of stroke outcome

All outcome assessments, including evaluation of ischemic infarction, brain water content and neurobehavioral performance were performed by investigators blinded to group assignments.

2.4.1. Behavioral tests and measurement of infarct volume and brain water content in SD rats

At 72 h after ischemia onset, the neurological behavioral tests were performed by investigator-blinded as previously described[23]. Neurological performance scores were assessed by using a five-point scale: 0, no significant deficits; 1, unable to stretch the left forepaw; 2, circling to the contralateral side; 3, reclining to the left side at rest; and 4, no spontaneous movement. After measure of neurological behavior, rats were sacrificed and brains were sectioned into 2-mm coronal slices. The sections were stained in phosphate buffer containing 2% TTC (Sigma−Aldrich) for 10 min at 37 °C. The brain infarction rates of the infarct volume to the total brain volume were calculated by using Image J. At 72 h post-ischemia, the brain water content was evaluated as previous described[24]. The water content rates of brain were calculated according to Eq. (1):

$$\text{Water content rate } (\%) = (\text{Wet weight} - \text{Dry weight})/\text{Wet weight} \times 100 \quad (1)$$

2.4.2. Measurement of infarct volume and brain edema volume in M. fascicularis

Magnetic resonance imaging (MRI) scans for the monkeys were performed before, at Day 3, and Day 7 after tMCAO. Anesthesia was induced by ketamine (10 mg/kg, IM) and maintained *via* intubation with isoflurane (1%−2%, oxygen flow at 0.6 L/min) (RWD Life Science Co., Ltd.). Then monkeys were immobilized in a prone position and placed in a Philips Achieva 3.0T MRI scanner (Philips, Amsterdam, The Netherlands). For measurement of infarct volume, Diffusion-weighted and Turbo Spin Echo (TSE) images were obtained. Diffusion-weighted images (DWI) were obtained from a 1.5 mm-thick axial and coronal section with 51.3 mm interval by using a 138 mm field of view (FOV), TE = 159 ms, TR = 10.2 ms, FA = 90° and reconstructed using a 184 × 182 image matrix. For measurement of brain edema volume, T2-weighted and Fluid attenuated inversion recovery (FLAIR) image were obtained. T2-weighted images (T2WI) were obtained from a 1.5 mm-thick axial and coronal section with 16.4 mm interval by using a 138 mm field of view (FOV), TE = 65 ms, TR = 3780 ms, FA = 90° and reconstructed using a 184 × 182 image matrix. The brain infarct volume and edema volume were calculated by investigator-blinded using RadiAnt DICOM Viewer software (version 4.6.5, Poznan, Poland). The results are represented with the ratio of brain infarction volume or edema volume to total brain volume.

2.4.3. Behavioral tests in M. fascicularis

The neurological function of monkeys was evaluated and recorded before and at 1, 3, 5, 7, and 14 days after tMCAO by investigator blinded using an examination scale as previous described[25]. The examination scale used in our study is shown in Supporting Information Table S1. Briefly, the state of consciousness, skeletal muscle coordination, sensory system, motor system was scored on an evaluation system with a maximum score of 100. A high score represented severe neurological deficit. On Day 14 post-ischemia, after neurological behavior test, the monkeys were euthanized and transcardially perfused with cold saline. The brain samples were collected and stored at −80 °C for further experiments.

2.5. In vivo BBB permeability

2.5.1. Evaluation of evans blue dye extravasation

BBB disruption was evaluated using Evans blue dye (Sigma−Aldrich) extravasation on the 72 h after tMCAO as described previously[24,26]. Briefly, 2% solution of Evans blue (Sigma−Aldrich) dissolved in sterile saline was injected through the rat tail vein at a dose of four mL/kg of body weight at 1 h before the rat were sacrificed. Before the rat brain samples were removed, rats were transcardially perfused with 100 mL of 0.9% cold saline to remove the intravascular dye. The brain sample were weighted, homogenized in 50% trichloroacetic acid solution (Sigma−Aldrich) diluted with saline and centrifuged at 12,000×*g* for 30 min. Then, the resultant supernatant was diluted 4-fold with ethanol and spectrophotometrically quantified at 620 nm to determine the extravasation of Evans blue dye (Sigma−Aldrich)

in a ThermoFisher plate-reader (Waltham, MA, USA; excitation at 620 nm and emission at 680 nm).

2.5.2. *Immunohistological detection of endogenous immunoglobulin G (IgG) extravasation*

BBB disruption could be also assessed through a one-step immunohistochemical detection of IgG[24]. The rats were transcardially perfused with PBS (pH 7.2 to 7.4, Beyotime) followed by ice-cold 4% paraformaldehyde (Servicebio, Wuhan, China). Then, rat brains were removed, post-fixed in 4% paraformaldehyde (Servicebio), cryoprotected in 15% and 30% sucrose in PBS (pH 7.2 to 7.4) (Beyotime) in turn for 2 days, and then sliced into 20 mm frozen sections on a freezing microtome (Leica, Japan). The sections were rinsed thrice with PBS (pH 7.2 to 7.4, Beyotime), followed by blocked with 10% normal goat serum (Vector Laboratories, Burlingame, CA, USA) for 1 h, and then the sections were incubated 1 h at room temperature with Alexa Fluor 488® conjugated goat anti-rat IgG (Abcam). After three rinses with PBS (pH 7.2 to 7.4, Beyotime) for 5 min each time, the fluorescent images were visualized with a VS200 Research Slide Scanner (Olympus, Tokyo, Japan), and the fluorescence intensity of lgG and area of lgG extravasation were measured by Image J software.

2.6. *Isolation and extraction of rat cerebral microvessels*

Rat cerebral microvessels were obtained following the protocols described previously[24]. Briefly, rat right brains were rapidly removed after euthanized by isoflurane (RWD Life Science Co., Ltd.), homogenized with a loosely fitting Dounce tissue grinder in ice-cold PBS (pH 7.2 to 7.4, Beyotime) and then centrifuged at 720×*g* for 5 min at 4 °C. Then the supernatant was discarded and the pellet was washed thrice by resuspension in PBS (pH 7.2 to 7.4, Beyotime), followed by centrifugation at 720×*g* for 5 min. The pellet was resuspended in PBS (pH 7.2 to 7.4) (Beyotime), then gently layered on top of a 16% dextran solution (Mr ~40,000 kDa, #31389; Sigma), and finally centrifuged again at 4500×*g* for 20 min at 4 °C. The pellet was collected, and resuspended in dextran and centrifuged again for another 20 min. A pellet containing enriched brain microvessels was collected and stored at −80 °C for further experiments. According to the standard procedure, the purity of rat cerebral microvessels was over 90% based on CD31 (Merck Millipore) immunofluorescence staining.

2.7. *Isolation and culture of primary rBMECs*

Isolation and culture of primary rBMECs were prepared from 3-week-old SD rats, as described previously[24]. Briefly, four young SD rats (about 3 weeks old) were sacrificed and the cortex of rat brains were isolated with forceps. The meninges were detached by carefully rolling the brains on a sterile blotting paper and the resulting meninges-free cerebral cortex were collected. Then, the cortex tissue was sequential digested by type II collagenase (final concentration at 1 mg/mL, collagenase from *Clostridium histolyticum*, C6885; Sigma) plus DNase I (final concentration at 20 mg/mL, Sigma−Aldrich) and collagenase/dispase (final concentration at 1 mg/mL, #10269638001; Sigma) plus DNase I (Sigma−Aldrich). After two-step enzyme digestion, rat brain microvascular endothelial cell clusters were plated on plastic dishes pre-coated with type I collagen (concentration at 50 μg/mL diluted with 0.02 mol/L acetic acid, #354236; Corning, NY, USA) and cultured in ECM (ScienCell™ Research Laboratories) supplement with puromycin (final concentration at 4 mg/mL, GM-040401; Genomeditech, Shanghai, China) at 37 °C in a sterile incubator of 95% air and 5% CO_2. After 48 h, the cell culture medium was changed to ECM (ScienCell™ Research Laboratories) medium without puromycin. Then the medium was changed the every 2−3 days. Cells were splited at 90% confluence with 0.25% trypsin (Invitrogen) supplement with 0.2% EDTA (Thermo Scientific) and used for further experiments. According to this protocol, more than 95% of cells were CD31 (Merck Millipore)-positive rBMECs which could be used for the following indicated experiments.

2.8. *Isolation and culture of primary rat astrocytes*

Rat primary astrocytes were isolated from newborn to 24 h-old wild-type SD pups as described previously[24,27]. Briefly, the whole rat brains were placed into ice cold HBSS (pH 7.2 to 7.4, Beyotime), the meninges and other non-cortical tissues of the rat pups were removed, and then the whole cortex was dissected. The cerebral cortices were digested in 0.25% trypsin (Invitrogen) and DNase I (Sigma−Aldrich) about 6 min at 37 °C, followed by addition of 20% volume of FBS (Clark Bioscience) to stop the digestion. The cortices were fully dissociated by pipetting and the cell suspension was filtered through a 70 μm mesh (WHB Scientific, Shanghai, China). Then the cells were transferred to 75 cm^2 PLL-coated flask (final concentration at 0.1 mg/mL, P2636; Sigma), and incubated at 37 °C in an atmosphere of 95% air and 5% CO_2. Half of the culture media were changed twice per week. After 7 days of culture, primary rat astrocytes were isolated from confluent primary glial cultures, with microglia and oligodendrocytes removed by shaking on the shaker at 180 rpm at 37 °C for 18 h. And then the culture medium was discarded and the cells were detached with 0.25% trypsin and subcultured by replating at low density. Cells reached confluence within 10 days after subculture, and 13 to 14-day-old astrocytes were used to construct the *in vitro* BBB model. At this point, more than 95% of cells were GFAP (Abcam)-positive astrocytes[24].

2.9. *Co-culture of primary rat brain microvascular endothelial cells and primary rat astrocytes*

The co-culture of rBMECs and primary rat astrocytes was conducted following the method described previously[28]. Briefly, astrocytes were seeded on the underside surface of transwell chamber (0.4 μm pore-size; Corning, NY, USA) with the chamber turned reversed. Astrocytes in chamber were cultured in DMEM/F12 medium (Invitrogen) for 24 h and then brain microvascular endothelial cells were seeded on the inner side of chamber pre-coated with type I collagen (Corning). The endothelial cells and astrocytes were co-cultured for further 4−6 days in ECM (ScienCell™ Research Laboratories).

2.10. *Drug treatment in cells and OGD/R experiment*

When primary rBMECs reached 80%−90% confluency, the cells were treated with LFHP-1c (1, 2, or 5 μmol/L) for 9 h. Then cells were washed with PBS (Beyotime) for three times, followed by culture in DMEM without glucose (GIBCO BRL, Grand Island, NY, USA). The cells were incubated in a hypoxic chamber (1% O_2, 5% CO_2 and 94% N_2; ThermoFisher, Waltham, MA, USA) for

4 h. After that, cells were treated with DMSO (Sigma−Aldrich) or LFHP-1c (1, 2, or 5 μmol/L) in ECM (ScienCell™ Research Laboratories) under normoxia conditions for another 3 h.

2.11. *In vitro BBB permeability*

At the time points of OGD onset, reoxygenation onset and 3 h after reperfusion onset, the trans-endothelial electrical resistance (TEER) across endothelial cells/astrocytes layers was measured by a voltage measuring electrodes (Millipore, Billerica, MA, USA). The values were presented as $\Omega \times cm^2$ culture chamber (Corning). At the end of reoxygenation period, fluorescein isothiocyanate (FITC)-dextran (40 kDa; Sigma−Aldrich) was added in the inner side of chamber with a final concentration of 1 mg/mL. The 30 μL of abluminal media was taken after 1, 2, three and 6 h, and the fluorescence was measured with excitation at 495 nm and emission at 520 nm.

For the detection of endothelial permeability, primary rBMECs were seeded on the inner side of chamber (Corning) pre-coated with type I collagen and further cultured for 4−6 days. After exposure to 4 h OGD and 3 h reoxygenation, FITC-dextran (40 kDa; Sigma−Aldrich) was added into the inner side of insert (final concentration at 1 mg/mL). After 1 h, 30 μL of abluminal media was taken and the fluorescence was measured.

2.12. *Mouse brain-derived endothelial cells.3 culture*

Mouse brain-derived endothelial cells.3 (bEnd.3), an immortalized murine endothelia cell line, were obtained from American Type Culture Collection (ATCC® CRL-2299™; Manassas, VA, USA) and cultured in DMEM (Invitrogen) with 10% FBS (Clark Bioscience), 100 U/mL penicillin (Beyotime) and 100 μg/mL streptomycin (Beyotime) at 37 °C with an atmosphere of 95% air and 5% CO_2.

2.13. *RNA interference*

The sequence of *Pgam5* siRNA #1 and *Pgam5* siRNA #2 were 5′-GGAGAAGACGAG UUGACAUTT-3′ and 5′-CCAUAGAGA CCACCGAUAUTT-3′, respectively. The sequence of *Nrf 2* siRNA was 5′-GAGGAUGGGAAACCUUACU-3′, and the sequence of scramble siRNA were 5′-ACGUGACACGUUCGGAGAA-3′. The siRNAs were purchased from GenePharma (Shanghai, China).

Primary rBMECs were grown on 24-well plates or 35 mm^2 dishes. *Pgam5* siRNA, scramble siRNA (GenePharma) and Lipofectamine™ 3000 Transfection Reagent (Invitrogen) were dissolved in Optimen I (Invitrogen), respectively, and then cultured at room temperature for 10 min. The above solutions were then added into the same volume of Lipofectamine™ 3000 Transfection Reagent (Invitrogen) and equilibrated at room temperature for about another 20 min. All the siRNA mixtures were added to the antibiotic-free medium and adjusted to a 200 nmol/L RNA final concentration according to the manufacturer's protocols. In our experiments, siRNAs were transfected into rBMECs cells for 36 h for subsequent experiments.

2.14. *Quantitative real-time reverse transcriptase polymerase chain reaction (qRT-PCR)*

To determine the levels of mRNA expression, total RNA was extracted from rBMECs and rat cerebral microvessels using Trizol reagent (Vazyme). Isolated RNA was reverse-transcribed into cDNA using cDNA synthesis kit (Vazyme) following the manufacturer's protocols. Quantitative PCR was performed using synthetic primers and SYBR Green (Vazyme) with a Stepone™ Software v2.3 Detection System (Life technologies corporation, Gaithersburg, MD, USA) according to the standard protocols. The primer pairs used in this study are shown in Supporting Information Table S2. The mRNA levels were normalized to 18S rRNA and calculated using $2^{-\Delta\Delta Ct}$ method and the data were presented as the fold change in related mRNA expression.

2.15. *Immunoprecipitation*

Primary rat brain microvascular endothelial cells (rBMECs) were incubated with DMSO (Sigma−Aldrich) or LFHP-1c (2 μmol/L) for 1 h, and subsequently lysed and suspended in cell lysis buffer (Beyotime) containing protease and phosphatase inhibitors (ThermoFisher). The cell lysates were centrifuged for 10 min at 14,000×*g* at 4 °C. About 10% of the supernatant of each tube was used for Western blotting as inputs. After preclearing the cell lysate with protein A/G agarose (Beyotime) at 4 °C for 3 h, beads were removed by centrifugation at 1000×*g* for 5 min at 4 °C. And then, the supernatant of homogenates was incubated with PGAM5 primary antibody (Santa Cruz Biotechnology) at 4 °C overnight, followed by addition of protein A/G agarose (Beyotime) at 4 °C for another 4−6 h. The immunoprecipitation agarose beads (Beyotime) were washed with cell lysis buffer (Beyotime) for five times, and then the SDS-PAGE sample loading buffer (Invitrogen) was added to each tube. The samples with the loading buffer were boiled and resolved on SDS-PAGE gel. The respective protein precipitates were identified by immunoblot analysis.

2.16. *In vitro proteome labeling, pull-down and target validation*

To validate the directly interacting cellular protein targets of LFHP-1c, a photoaffinity probe HP-62 in which a photosensitive diazirine moiety was introduced to the acetyl group in LFHP-1c, was designed and synthesized (Supporting Information Scheme S1 and Fig. S2), and pull-down experiments were carried out, followed by immunoblotting. The general pull-down experiments were based on previously reported protocols[27] with some optimizations. Briefly, the primary rBMECs were washed thrice with PBS, and lysed with RIPA Lysis and Extraction Buffer (ThermoFisher) containing protease and phosphatase inhibitor (ThermoFisher) on ice for 30 min. A soluble protein solution was collected by centrifugation at 12,000×*g* for 20 min at 4 °C. Then the protein concentrations were determined by using the Pierce™ BCA Protein Assay Kit (ThermoFisher) and diluted to 1.5 μg/μL with RIPA Lysis and Extraction Buffer (ThermoFisher). Eventually, the 450 μg protein in 300 μL RIPA Lysis and Extraction Buffer (ThermoFisher) containing protease and phosphatase inhibitor (ThermoFisher) was added with DMSO (Sigma−Aldrich) or HP-62 (2 μmol/L), then the mixture was incubated for 9 h at 4 °C and followed by UV-irradiated (365 nm) for 30 min. A freshly pre-mixed click chemistry reaction cocktail (30 μmol/L Biotin-PEG_3-N_3 from 100 mmol/L stock solution in DMSO, 100 μmol/L TBTA from 100 mmol/L freshly prepared stock solution in DMSO, 1 mmol/L TCEP from 1 mol/L freshly prepared stock solution in deionized water, and 1 mmol/L $CuSO_4$ from 1 mol/L freshly prepared stock solution in deionized water) was added to the labeled proteome. The

reaction was further incubated for 2 h at room temperature prior to addition of pre-chilled acetone at −20 °C (Sigma−Aldrich). The precipitated proteins were subsequently collected by centrifugation at 14,000 × rpm for 10 min at 4 °C, and washed thrice with one mL of prechilled methanol at −20 °C (Sigma −Aldrich), the precipitated proteins were dissolved in PBS (Beyotime) containing 1% SDS. Upon incubation with Streptavidin Mag Sepharose™ pre-balanced with binding buffer (50 mmol/L Tris−HCl, 150 mmol/L NaCl, pH 7.5; GE Healthcare) by using the MagRack 6 (GE Healthcare) for 2 h at room temperature, then the magnetic sepharose beads were washed with PBS (Beyotime) containing 1% SDS (3 × 1 mL) and washing buffer (binding buffer containing 2 mol/L urea, pH 7.5; 3 × 1 mL). Finally, the enriched proteins were eluted by Novex™ Tris-Glycine SDS Sample Buffer (2×; Invitrogen) at 95 °C for 10 min and separated by SDS-PAGE (10%) and followed by immunoblotting.

2.17. Immunoblotting

Cytoplasmic, mitochondria and nuclear proteins were extracted with commercial kits (Beyotime) according to the manufactory instructions. The protein samples were obtained from cells, brain microvessels or brain cortex of *M. fascicularis* using RIPA buffer (Beyotime, Shanghai, China) containing Pierce Protease and Phosphatase Inhibitor Mini Tablets (EDTA-free; ThermoFisher). The extracted proteins were quantified by Pierce™ BCA Protein Assay Kit (ThermoFisher) and then equal amounts of proteins were separated by SDS-PAGE gels, followed by transferred to PVDF filter membrane (Millipore). The membranes were blocked with 3% BSA for 2 h at room temperature and then incubated overnight at 4 °C with primary antibodies against ZO-1 (1:1000; Proteintech Group), occludin (1:1000; Proteintech Group), VCAM-1 (1:1000; Abclonal), NRF2 (1:1000; Santa Cruz Biotechnology), HO-1 (1:500; Abcam Cambridge) for rat brain microvessels and brain cortex of *M. fascicularis* protein samples, HO-1 (1:1000; Proteintech Group) for rBMECs protein samples, PGAM5 (1:1000; ABclonal) for immunoblotting, p-DRP1 (Ser 637; 1:500, Cell Signal Technology) for rat protein samples, p-DRP1 (Ser637; 1:500, Affinity Biosciences) for brain cortex of *M. fascicularis* protein samples, PGAM5 (1:50; Santa Cruz Biotechnology) for co-immunoprecipitation, claudin-5 (1:1000, Affinity Biosciences), α-tubulin (1:5000; ABclonal), COXIV (1:1000; ABclonal), β-actin (1:5000; ABclonal), GAPDH (1:1000; ABclonal), H3 (1:1000; ABclonal) and LAMB1 (1:1000; Proteintech Group). After washing for five times with 6 min for each time, the membranes were incubated with secondary antibodies for another 1 h at room temperature. Then the membranes were washed for another five times and the proteins were visualized with ChemiDoc System (Bio-Rad, Hercules, CA, USA). And the bands were quantified by ImageJ software.

2.18. Confocal imaging

The endothelial cells were washed with PBS (Beyotime) for three times and then fixed with 4% paraformaldehyde (Servicebio) for 30 min. After that, the cells were blocked with 10% normal goat serum (Vector Laboratories) for 1 h, followed by incubation with rabbit anti-ZO-1 (1:250, Proteintech), CD31 (1:250, Merck Millipore), GFAP (1:500, Abcam) overnight at 4 °C. Then cells were further incubated with Alexa Fluor 488® conjugated goat anti-rabbit secondary antibody (1:500, Invitrogen) or Alexa Fluor 633® conjugated goat anti-mouse secondary antibody (1:500, Invitrogen). Hoechst 33342 (Beyotime) was utilized to label cell nuclei. The fluorescent images were photographed with Olympus fluorescence FV 3000 microscope (Olympus, Tokyo, Japan) and the fluorescence intensity was measured using Image J.

Rat brain microvessel pellet was prepared in the same manner as above, followed by freezing in isopentane on dry ice. Frozen rat brain microvessel pellet was cut individually into 14-mm thick consecutive sections in a Cryostat (Leica, Germany) at −20 °C. The sections were thawmounted onto gelatin-coated glass slides. Then, the sections were fixed with 4% paraformaldehyde for 1 h, followed by incubation in a blocking solution containing 10% normal goat serum (Vector Laboratories) and 0.1% Triton X-100 (Sangon Biotech, Shanghai, China) in PBS (Beyotime) at room temperature. Next, the sections were incubated with mouse anti-CD31 (1:100, Merck Millipore) overnight at 4 °C. Then, the samples were incubated with Alexa Fluor 633® conjugated goat anti-mouse secondary antibody (1:500, Invitrogen) and counterstained with Hoechst 33342 (Beyotime) to label all cell nuclei. The fluorescent images were photographed with Olympus fluorescence FV 3000 microscope (Olympus).

2.19. LDH assay

The effect of LFHP-1c on endothelial cells viability was evaluated by LDH assay through a commercial LDH Cytotoxicity Assay Kit (Beyotime). After LFHP-1c and/or OGD treatment, the culture medium samples were transferred into an optically clear 96-well plate and 60 μL Reaction Mix was added according to the manufacturer's recommendations. After 3−5 min incubation at 37 °C, absorbance was measured at 490 nm.

2.20. Surface plasmon resonance (SPR) assay

In order to verify whether LFHP-1c could bind with PGAM5, SPR, the most recognized method for studying the dynamic properties between ligands and donors, was used. In this experiment, we refer to previously published protocols with some optimizations[27]. Briefly, 10 μmol/L LFHP-1c in PBS (Beyotime) was printed on the 3D photo-crosslinking chip (BetterWays, Inc.) *via* the Biodot™ AD1520 chip array printer (BioDot Corporation) through C−H covalent bond connection, and then different concentrations of purified recombinant protein ΔN21-PGAM5 flowed through the surface of the chip at 0.5 μL/s in PBS-P (pH 7.4; 28-9950-84; GE Healthcare, Buckinghamshire, UK) for 600 s at 25 °C. Finally, the proteins were dissociated from the chip at two μL/s in glycine-HCl (pH 2.0) for 360 s at 25 °C. The binding signals (RU) were detected by SPR using Biacore 3000 (GE Healthcare, Pittsburgh, PA, USA). The RU responses of LFHP-1c with ΔN21-PGAM5 were recorded and ranked, and the binding curve and affinity data were calculated by the system according to the Langmuir binding model.

2.21. Statistical analysis

All statistical analyses were performed using GraphPad Prism eight Software (La Jolla, CA, USA). All results are presented as mean ± standard error of mean (SEM). For data with a single dosage or time point, the differences between groups were

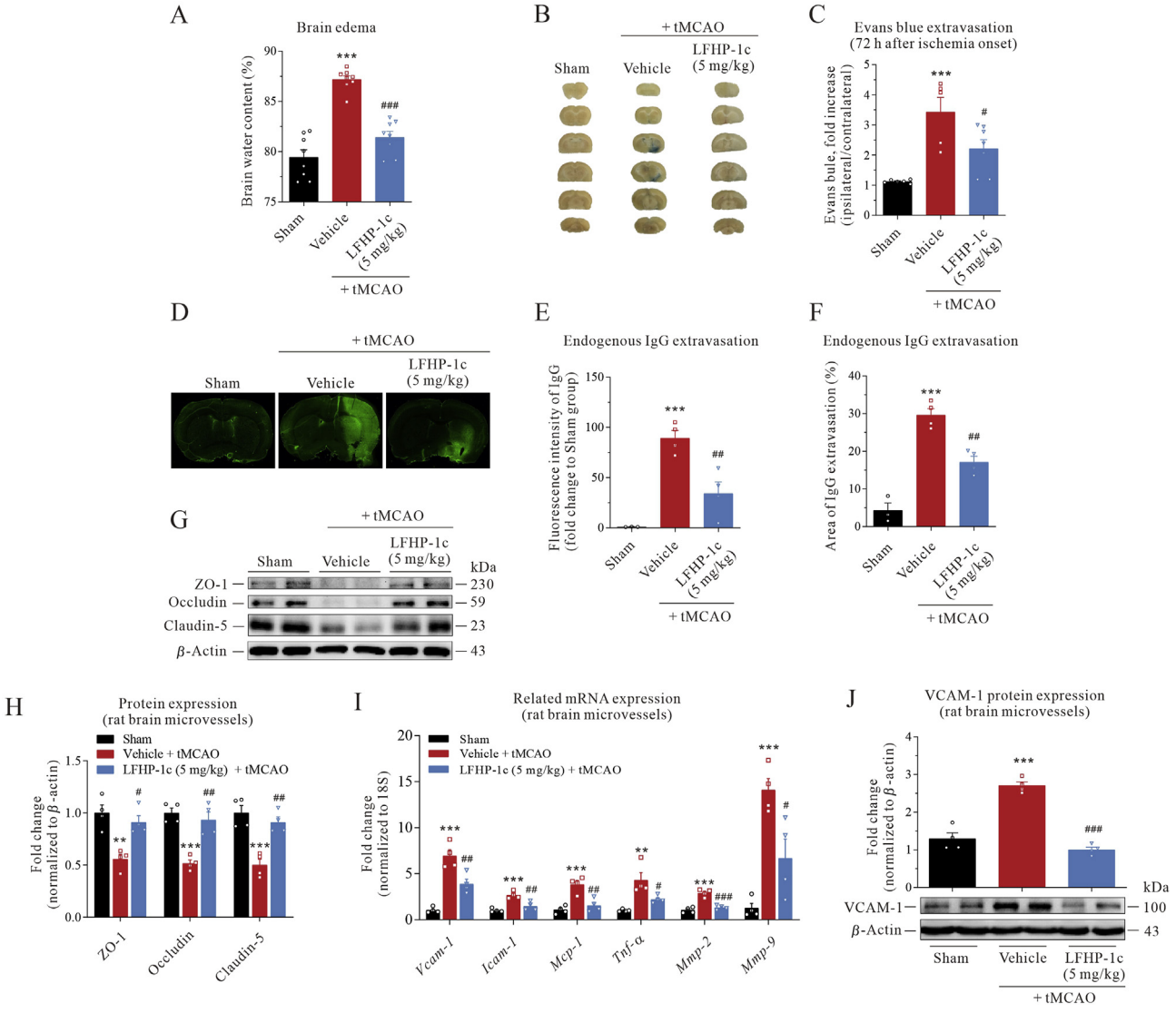

Figure 1 LFHP-1c attenuates brain edema, protects BBB integrity and attenuates brain microvascular endothelial inflammation in rats at 72 h after ischemia onset. (A) When administered at four and 24 h after tMCAO, LFHP-1c (5 mg/kg) attenuated tMCAO-induced brain edema at 72 h post-ischemia, $n = 8$ per group. (B) and (C) When administered at 4 h after tMCAO, LFHP-1c (5 mg/kg) attenuated tMCAO-induced Evans blue leakage in the brain of rats, $n = 5-7$ per group. (D)−(F) Post-ischemic treatment with LFHP-1c (5 mg/kg) reduced the content and area of endogenous IgG extravasation to brain tissue, $n = 3-4$ per group. The scale bar represents 1 mm. (G) and (H) LFHP-1c treatment prevented tMCAO-induced degradation of tight junction proteins ZO-1, occludin and claudin-5 in isolated rat brain microvessels at 72 h post-ischemia, $n = 4$ per group. (I) Post-ischemic treatment with LFHP-1c attenuated mRNA expression of *Vcam-1*, *Icam-1*, *Mcp-1*, *Tnf-α*, *Mmp 2* and *Mmp 9* in isolated rat brain microvessels at 72 h post-ischemia, $n = 4$ per group. (J) LFHP-1c alleviated the protein expression of VCAM-1 in isolated rat brain microvessels at 72 h post-ischemia, $n = 4$ per group. Results are expressed as mean ± SEM. $^{**}P < 0.01$, $^{***}P < 0.001$ *versus* Sham group; $^{\#}P < 0.05$, $^{\#\#}P < 0.01$, $^{\#\#\#}P < 0.001$ *versus* Vehicle group.

analyzed by one-way ANOVA with Bonferroni's test. The *t*-test was used for comparison between two groups, including *in vivo* evaluation of LFHP-1c with various doses or administration at different times on cerebral ischemic and neurological deficits at 72 h after ischemia onset. Two-way ANOVAs followed by Bonferroni's test were utilized for multi-factors comparisons of the parameters including *Pgam5* siRNA, NRF2 siRNA, co-immunoprecipitation and the nuclear translocation of NRF2 after knockdown of *Pgam5* experiments. The differences in Longa test were analyzed by non-parametric Mann−Whitney test. A P value of 0.05 or less was considered statistically significant.

3. Results

3.1. LFHP-1c dose-dependently protects rat brains against ischemia/reperfusion injury at 72 h after ischemia onset with a moderate therapeutic window

To determine whether LFHP-1c protects against ischemia/reperfusion-induced neurological injury in a dose-dependent manner, rats were subjected to tMCAO model and were administrated with vehicle or LFHP-1c at four and 24 h after ischemia onset, and neurologic deficits and brain infarcts were assessed at

72 h post-ischemia (Supporting Information Fig. S3A). As shown in Fig. S3B and S3C, compared to vehicle, the treatment of LFHP-1c significantly decreased brain infarct volume in a dose-dependent manner. Moreover, administration with LFHP-1c significantly ameliorated neurological deficits in a dose-dependent manner compared to vehicle (Fig. S3D).

To determine the therapeutic window of LFHP-1c, the rats were administrated with LFHP-1c (5 mg/kg) at four or 12 h after ischemia onset, respectively, and then another time at 24 h post-ischemia (Fig. S3E). As shown in Fig. S3F and S3G, LFHP-1c significantly attenuated brain infarct volume in rats even treated at 12 h post-ischemia compared to the vehicle group. And neurological deficits were improved in LFHP-1c group compared to vehicle group (Fig. S3H). Besides, rats administrated with LFHP-1c (5 mg/kg) at four and 24 h exerted better neurological recovery than that at 12 and 24 h (Fig. S3H). Furthermore, rats in the LFHP-1c group (5 mg/kg, four and 24 h) showed significantly decrease in brain water content (Fig. 1A). Moreover, administration with LFHP-1c (5 mg/kg) did not affect rat blood pressure (Fig. S3I). These results indicate that LFHP-1c decreased brain infarct volume and brain edema, and improved neurological deficits after tMCAO injury, without any alteration of blood pressure.

3.2. *LFHP-1c prevents BBB disruption and attenuates endothelial inflammation in rat cerebral microvessels at 72 h after ischemia onset*

To assess the BBB permeability after ischemia/reperfusion injury, Evans blue and endogenous IgG extravasation were detected in the rat brain. As shown in Fig. 1B and C, Evans blue leakage in vehicle group was increased at 72 h post-ischemia compared to the sham group, and LFHP-1c (5 mg/kg) significantly reduced Evans blue content in brain tissue. Data in Fig. 1D−F show that post-ischemic administration with LFHP-1c significantly attenuated IgG content and extravasation area in the rat brain compared to the vehicle group. These data indicate that LFHP-1c improved BBB integrity after tMCAO damage.

It has been reported that tight junction proteins between endothelial cells, notably zonula occludens-1 (ZO-1), occludin and claudin-5 contributed to the BBB integrity after ischemia-induced brain injury[29]. Accordingly, we assessed the expression of tight junction proteins ZO-1, occludin and claudin-5 in isolated rat brain microvessels at 72 h after onset of ischemia. As shown in Fig. 1G and H, the protein expressions of ZO-1, occludin and claudin-5 significantly decreased in vehicle group, while LFHP-1c administration reversed this effect.

The expression of endothelial adhesion molecules (VCAM-1, ICAM-1) and monocyte chemoattractant protein-1 (MCP-1) is crucial for the recruitment of leukocytes to the damage sites after ischemia injury, which would aggravate BBB disruption and ischemic injury. Also, MMPs contribute to the degradation of tight junction proteins in response to ischemia. Thus, we detected the gene expression of endothelial inflammation factors at 72 h post-ischemia injury in isolated rat brain microvessels through RT-PCR. As shown in Fig. 1I, LFHP-1c significantly attenuated the mRNA expression of intercellular adhesion molecule 1 (*Icam-1*), vascular cell adhesion molecule 1 (*Vcam-1*), *Mcp-1*, *Tnf-α*, *Mmp 2* and *Mmp 9* compared to vehicle group. Furthermore, LFHP-1c significantly decreased the protein expression level of VCAM-1 in isolated rat brain microvessels (Fig. 1J). These results suggest that LFHP-1c treatment ameliorated tMCAO-induced brain microvascular endothelial inflammation.

3.3. *LFHP-1c prevents primary rBMECs injury under OGD/R condition*

To further study the effect of LFHP-1c on BBB protection, we established an *in vitro* BBB model by co-culture of primary rBMECs (Supporting Information Fig. S4A) and primary rat astrocytes (Fig. S4B) as previously reported[24], and the TEER and FITC-dextran permeability were applied to assess BBB integrity in this study (Fig. 2A). As shown in Fig. 2B, OGD/R significantly decreased TEER values at the time points of reoxygenation onset and 3 h after reoxygenation (Fig. 2B), while LFHP-1c significantly increased TEER values at the time points of reoxygenation onset and 3 h after reoxygenation (Fig. 2B). Also, OGD/R significantly increased FITC-dextran flux in co-culture of rBMECs and astrocytes (Fig. 2C), while LFHP-1c decreased FITC-dextran flux (Fig. 2C). Furthermore, LFHP-1c also significantly decreased FITC-dextran flux across the monolayer of endothelia cells compared to the OGD/R group (Fig. 2D). Next, we further investigated the effects of various concentrations of LFHP-1c on viability of endothelia cells exposed to OGD/R injury, and the data in Fig. 2E show that LDH release in rBMECs was significantly increased after OGD/R injury, which was remarkably attenuated by LFHP-1c treatment. TUNEL assay was utilized to stain apoptotic cells after OGD/R injury. As shown in Fig. 2F and G, LFHP-1c significantly reduced apoptosis in rBMECs after OGD/R-induced damage. Moreover, the expressions of tight junction proteins ZO-1, occludin and claudin-5 in rBMECs were upregulated in LFHP-1c-treated groups compared to the OGD/R group (Fig. 2H and I). Furthermore, the results of immunofluorescence staining of ZO-1 in rBMECs suggest that LFHP-1c prevented the degradation of tight junction protein ZO-1 in endothelial cells after OGD/R injury (Fig. 2J and K). Additionally, LFHP-1c also attenuated OGD/R-induced upregulation of endothelial adhesion molecule *Vcam-1* gene expression (Fig. 2L) and VCAM-1 protein expression (Fig. 2M). These results suggest that LFHP-1c protected brain microvascular endothelial cells, which may contribute to the BBB protection of LFHP-1c in rats with tMCAO.

3.4. *PGAM5 protein is a key target of LFHP-1c in endothelia cells*

To identify the direct target proteins of LFHP-1c which are responsible for its BBB protection, SPR and liquid chromatography−mass spectrometry/mass spectrometry (LC−MS/MS) analysis were performed to capture target proteins of LFHP-1c in endothelial cells. The experiment flow is showed in Fig. 3A. LFHP-1c was printed on the 3D photo-crosslinking chip *via* the chip array printer through C−H covalent bond connection, and then the lysates of endothelial cells flowed through the surface of the chip. Finally, the proteins were collected by dissociation from the chip, analyzed by LC−MS/MS, and then compared with UniProt database. The possible target proteins captured by LFHP-1c were showed in Supporting Information Table S3. Previous studies in our group have shown that LFHP-1c switched microglia from pro-inflammatory phenotype to anti-inflammatory phenotype through activating NRF2, and thus protecting cerebral ischemia[21]. Therefore, we searched the possible target proteins associated with NRF2, and a target protein candidate, PGAM5, appeared in our interest (Table S3). In order to conduct follow-up experiments, two kinds of PGAM5 recombinant proteins, ΔN21 PGAM5 (residues 22−289 aa) and ΔN90 PGAM5 (residues 91−289 aa), were expressed and

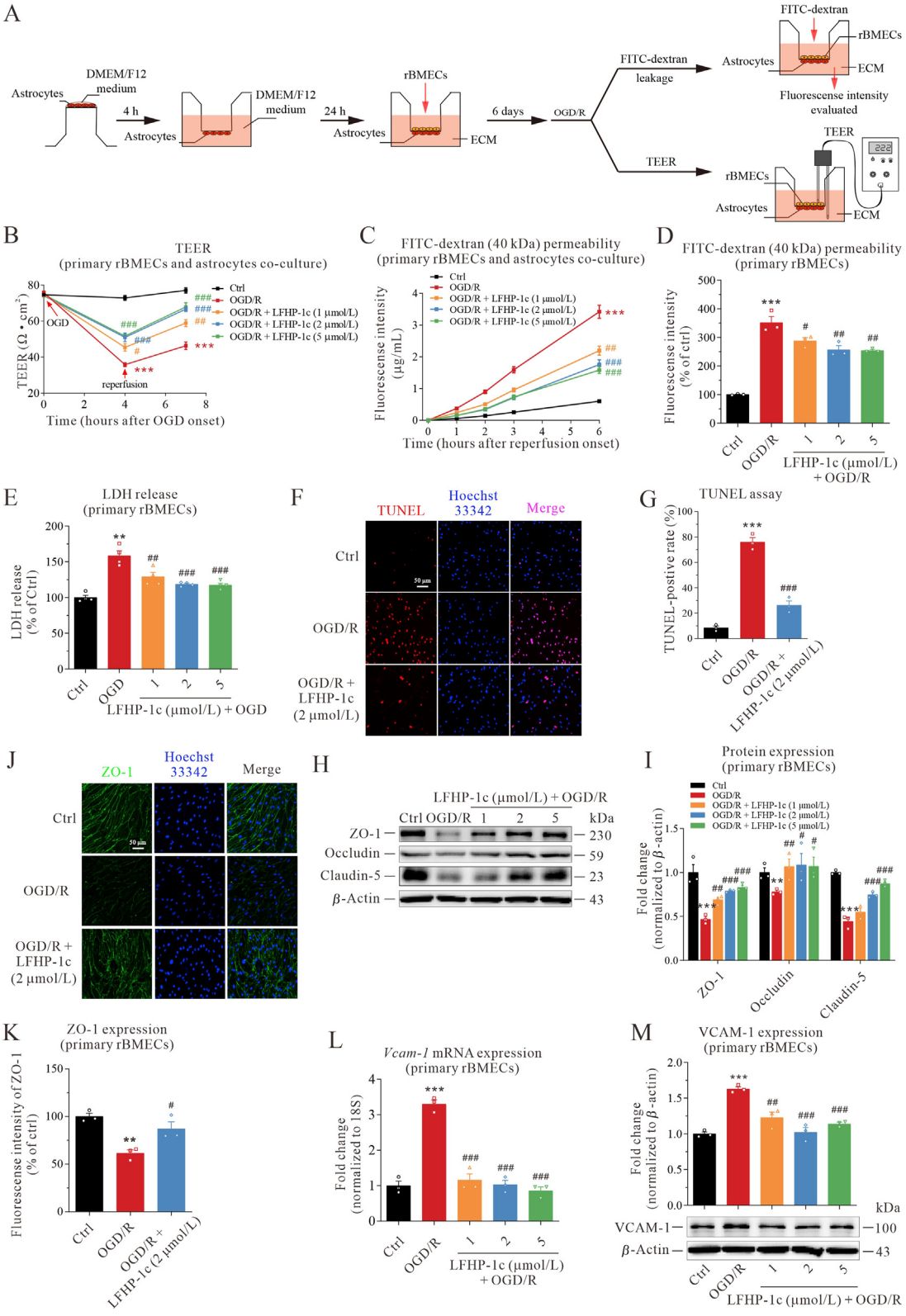

Figure 2 LFHP-1c prevents brain microvascular endothelial cells injury under OGD/R condition. (A) Schematic illustration of *in vitro* BBB model. The *in vitro* BBB model was established with co-culture of primary rat brain microvascular endothelial cells and primary rat astrocytes. After exposure to OGD/R injury, the *in vitro* BBB disruption was assessed by FITC-dextran permeability and TEER. (B) The *in vitro* BBB model was pretreated with LFHP-1c (1, two or 5 μmol/L) for 9 h, followed by exposed to 4 h OGD and 3 h reoxygenation, and TEER was measured at the time points of OGD onset, reoxygenation onset and the end of reoxygenation, $n = 3$ per group. (C) FITC-dextran (40 kDa) permeability across the *in vitro* BBB model was measured at 1, 2, three and 6 h after the end of reoxygenation period, $n = 3$ per group. (D) FITC-dextran

purified in our laboratory (Supporting Information Fig. S5A). In according with previous reports[6,7], only ΔN21 PGAM5 (residues 22−289 aa) exhibited phosphatase activity in PGAM5 enzyme assay (Fig. S5B), and thus ΔN21 PGAM5 (residues 22−289 aa) was used for SPR and phosphatase activity assay. SPR is a spectroscopic technique that monitors the changes in refractive index at the interface of a liquid sample and a surface with an immobilized sensor molecule and the binding signal was shifted as a result of analyte binding or induced protein conformational changes. SPR, which is the most recognized method for studying the dynamic properties between ligands and donors now, was used to detect whether LFHP-1c could directly bind with PGAM5. The SPR results suggest that there was a strong binding between LFHP-1c and PGAM5 with the K_D value of about 0.961 μmol/L (Fig. 3B). We then tested whether LFHP-1c could inhibit the phosphatase activity of PGAM5, and the results indicate that LFHP-1c significantly inhibited PGAM5 phosphatase activity in a concentration-dependent manner (Fig. 3C). LFHP-1c also concentration-dependently inhibited PGAM5 phosphatase activity in isolated mitochondria from endothelia cells (Fig. 3D and Supporting Information Fig. S6). Furthermore, we designed and synthesized a photoaffinity probe, HP-62 to further confirm the direct binding of LFHP-1c with PGAM5 in endothelia cells. The synthetic route of HP-62 was depicted in Scheme S1 and the workflow chart of protein target identifications was shown in Fig. 3E. A diazirine group bearing an azide moiety was introduced to the acetyl moiety of LFHP-1c to obtain a photoaffinity probe HP-62. Once activated by UV irradiation, diazirine group generates highly reactive carbene species, which formed covalent bonds through addition reactions with amino acid side chains in the binding proteins[30]. The copper-catalyzed alkyne−azide cycloaddition (CuAAC) "click" reaction of the terminal azide moiety was utilized for further biotin streptavidin based proteins enrichment[27,31]. As shown in Fig. 3F, we evaluated the photoaffinity probe HP-62 effect on PGAM5 phosphatase activity as compared to that of the parent compound (LFHP-1c) in phosphatase activity assay, and the results reveal that HP-62 retained the PGAM5 phosphatase activity the same as LFHP-1c and HP-62 could be used for subsequent experiments. To further study whether LFHP-1c could bind with PGAM5 directly in endothelia cells, we used HP-62 to label the macromolecular binding partners and enriched the target proteins that possibly bind with LFHP-1c. The labeling was done through click reaction between HP-62 and biotin-PEG_3-N_3, followed by affinity enrichment (Fig. 3E). The proteins labeled by HP-62, followed by enriched by streptavidin beads, were used for Western blotting using the corresponding antibodies. As shown in Fig. 3G, LFHP-1c probe HP-62 directly binds with PGAM5. All these results above indicate that PGAM5 protein is an important key target of LFHP-1c in endothelia cells and may contribute to the BBB protection of LFHP-1c.

3.5. *LFHP-1c targets PGAM5 to facilitate nuclear translocation of NRF2 for endothelial protection in stroke*

Our previous study has described that LFHP-1c promotes NRF2 activation in microglia to exert anti-neuroinflammatory effect, but whether LFHP-1c activates NRF2 in endothelial cells remains unclear. As shown in Fig. 4A and Supporting Information Fig. S7C, LFHP-1c could increase NRF2 protein expression in rBMECs. Moreover, LFHP-1c significantly upregulated the protein expression of heme oxygenase-1 (HO-1) (Fig. 4A and Fig. S7D) and mRNA expression of *Ho-1* and NAD(P)H dehydrogenase [quinone] 1 (*Nqo1*) (Fig. S7E and S7F) in rBMECs. Also, LFHP-1c treatment showed no effects on PGAM5 expression (Fig. 4A and Fig. S7A), but significantly upregulated the expression of PGAM5 substrate DRP1 phosphorylation at Ser 637 site (p-DRP1, Ser 637) in cultured rBMECs (Fig. 4A and Fig. S7B). It has been reported that NRF2 forms a complex with a KEAP1 dimmer and PGAM5[16]. Due to LFHP-1c directly binding with PGAM5 in rBMECs, we proposed a hypothesis that LFHP-1c inhibits the interaction between PGAM5 and NRF2. The IP and Western blotting results reveal that LFHP-1c treatment significantly reduced the interaction of PGAM5 with NRF2 (Fig. 4B and C). As shown in Fig. 4D, LFHP-1c facilitated nuclear translocation of NRF2 in rBMECs. Moreover, we found that knockdown of *Pgam5* also promoted nuclear translocation of NRF2, which is similar as LFHP-1c treatment, but the enhanced NRF2 nuclear translocation by LFHP-1c treatment was not affected by knockdown of *Pgam5* (Fig. 4E−G), which has been also demonstrated by the immunofluorescence staining of NRF2 in rBMECs (Fig. 4H). These results above suggest that LFHP-1c may target PGAM5 to facilitate nuclear translocation of NRF2 for endothelial protection and BBB integrity in stroke model.

3.6. *LFHP-1c regulates PGAM5−NRF2 axis in rat cerebral microvessels isolated from rats at 72 h after tMCAO onset*

To verify the molecular mechanism of LFHP-1c on endothelial protection, we further examined the effect of LFHP-1c on PGAM5−NRF2 axis in isolated rat cerebral microvessels at 72 h post-ischemia. Increased PGAM5 expression and decreased phosphorylation of DRP1 at Ser 637 site were observed after subjected to tMCAO compared to the sham group (Fig. 4I and J), and the upregulated PGAM5 expression and down-regulation of phosphorylation of DRP1 at Ser637 site induced by ischemia were attenuated by LFHP-1c treatment (Fig. 4I and J). Furthermore, LFHP-1c enhanced NRF2 expression and stimulated HO-1 expression (Fig. 4I and J) at protein level in isolated rat cerebral microvessels. In addition, LFHP-1c enhanced the

(40 kDa) permeability across the rBMECs monolayer was measured at 1 h after the end of reoxygenation, $n = 3$ per group. (E) rBMECs were treated with LFHP-1c (1, two or 5 μmol/L) for 9 h, then exposed to OGD injury for 4 h, and the content of LDH release to culture medium was measured, $n = 4$ per group. (F) and (G) TUNEL staining shows that pretreated with LFHP-1c reduced apoptosis in rBMECs after OGD/R injury, $n = 3$ per group. The scale bar represents 50 μm. (H) and (I) LFHP-1c prevented the degradation of tight junction proteins ZO-1, occludin and claudin-5 induced by OGD/R, $n = 3$ per group. (J) and (K) Fluorescence staining of ZO-1 shows that LFHP-1c improved ZO-1 expression after OGD/R injury, $n = 3$ per group. The scale bar represents 50 μm. (L) and (M) LFHP-1c reduced the expression of *Vcam*-1 mRNA (L) and VCAM-1 protein (M) after exposure to OGD/R, $n = 3$ per group. Results are expressed as mean ± SEM. For Fig. 3B−D and Fig. 3F to M: $^{**}P < 0.01$, $^{***}P < 0.001$ *versus* Control (Ctrl) group; $^{\#}P < 0.05$, $^{\#\#}P < 0.01$, $^{\#\#\#}P < 0.001$ *versus* OGD/R group. For Fig. 3E: $^{**}P < 0.01$ *versus* Control (Ctrl) group; $^{\#\#}P < 0.01$, $^{\#\#\#}P < 0.001$ *versus* OGD group.

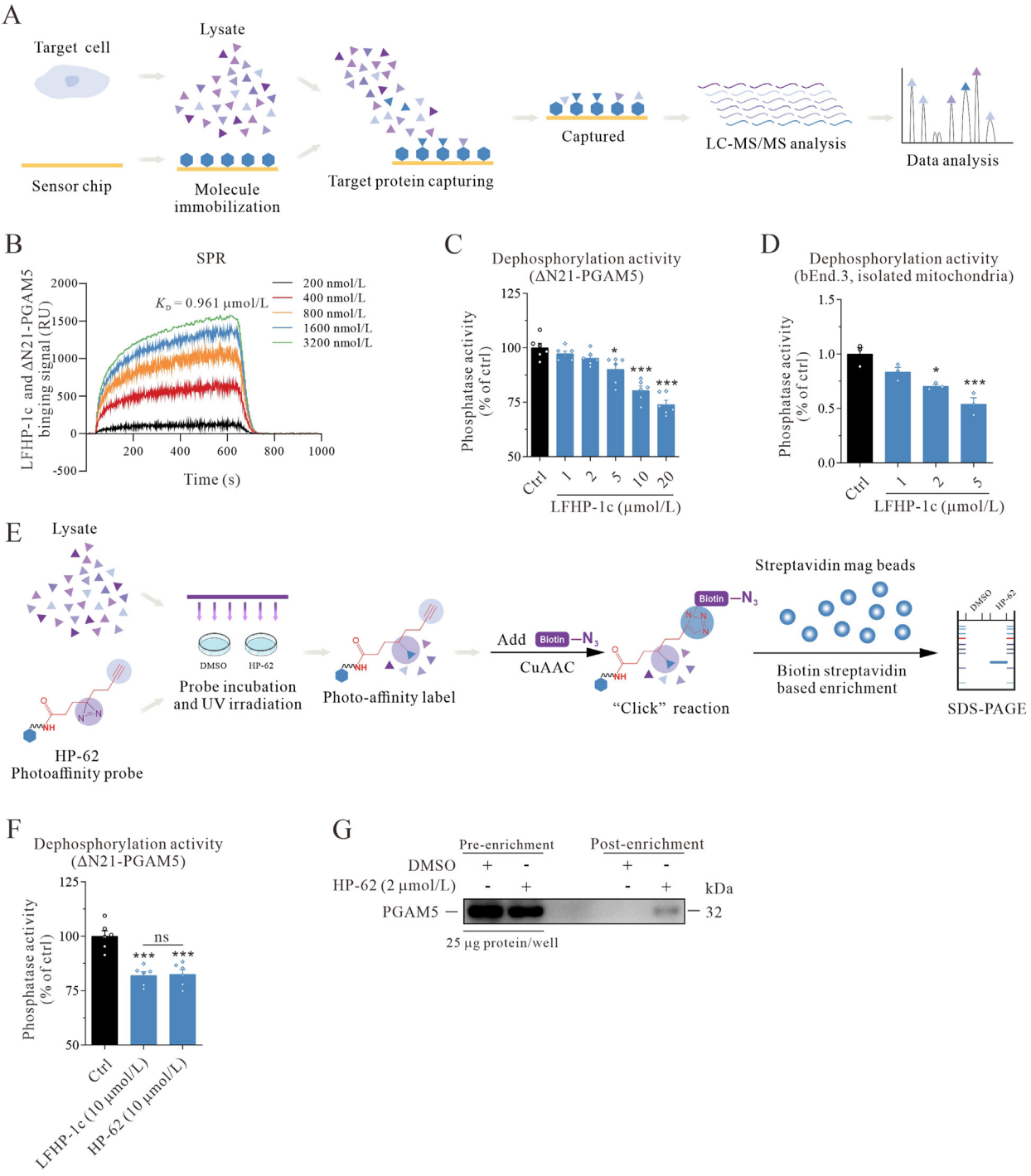

Figure 3 Target verification of LFHP-1c in endothelial cells. (A) Schematic illustration of target protein capture of LFHP-1c in endothelial cells based on SPR. LFHP-1c was printed on the 3D photo-crosslinking chip *via* the chip array printer through C−H covalent bond connection, and then the lysates of endothelial cells flowed through the surface of the chip. Finally, the proteins were dissociated from the chip and conducted LC−MS/MS analysis and compared with UniProt database. (B) LFHP-1c binds with ΔN21-PGAM5 in kinetic level determined by SPR, and the K_D value was about 0.961 μmol/L. (C) LFHP-1c concentration-dependently inhibited the dephosphorylation activity of ΔN21-PGAM5 at molecular level, $n = 6$ per group. (D) LFHP-1c inhibited the dephosphorylation activity of PGAM5 in isolated mitochondria from mouse brain-derived Endothelial cells.3 (bEnd.3) in a concentration-dependent manner, $n = 3$ per group. (E) Schematic illustration of target identification in rBMECs lysates. Photoaffinity probe HP-62 binds with proteome in rBMECs through photoaffinity labeling, and then clicks with biotin-PEG3-N3 based on copper-catalyzed azide−alkyne cycloaddition (CuAAC), subsequently enriched by Streptavidin Mag Sepharose™ beads, and finally separated by SDS-PAGE followed by immunoblotting. (F) Evaluation of HP-62 effect on the dephosphorylation activity of PGAM5 compared to the parent compound LFHP-1c at molecular level, and the results reveal that HP-62 retained the dephosphorylation activity of PGAM5, $n = 6$ per group. (G) Pull-down/Western blotting for target validation of PGAM5 with the photoaffinity probe HP-62, and a representative blot shown here. Results are expressed as mean ± SEM. $^*P < 0.05$, $^{***}P < 0.001$ *versus* Control (Ctrl) group.

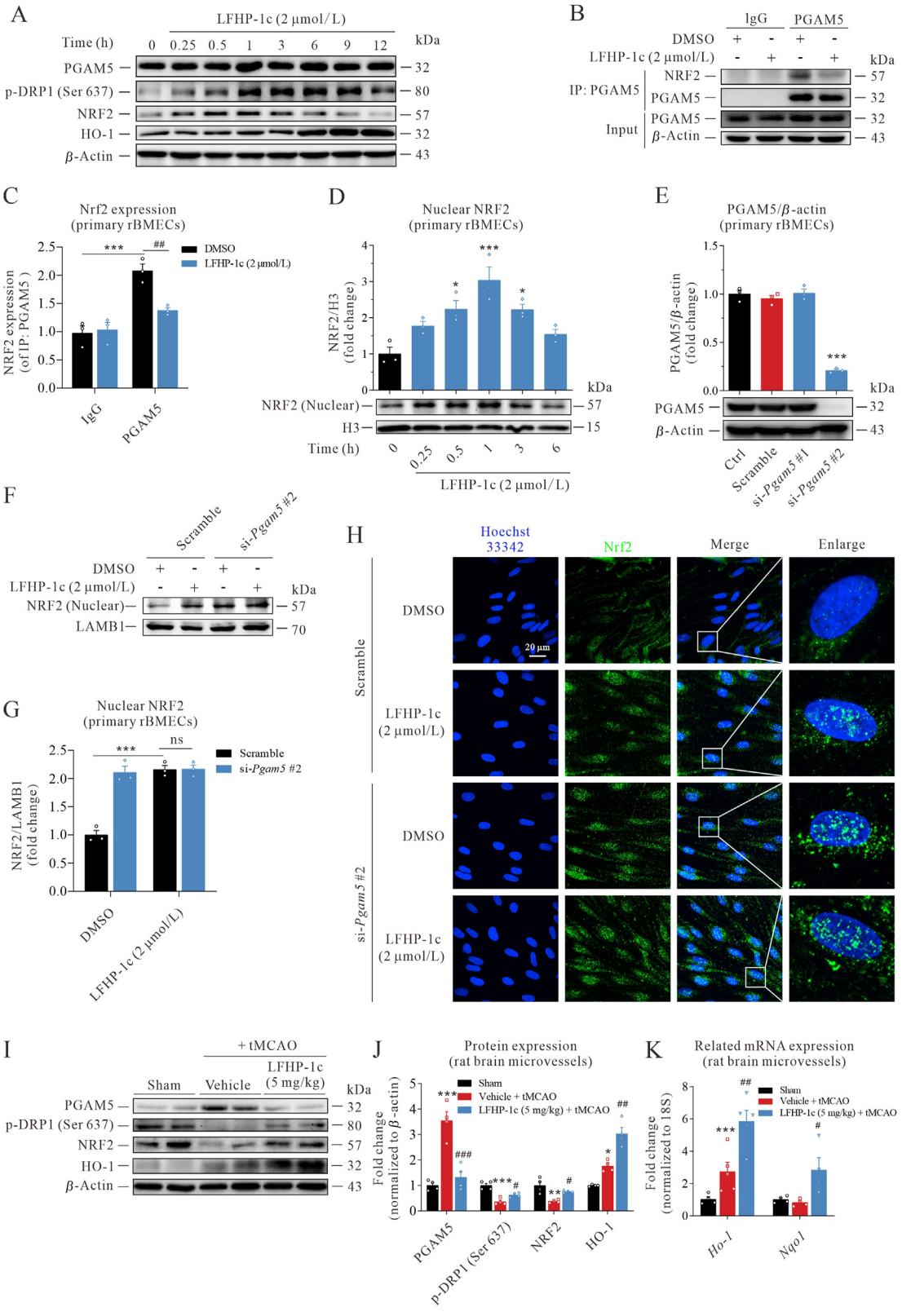

Figure 4 LFHP-1c targets PGAM5 to facilitate nuclear translocation of NRF2 for endothelial protection in stroke. (A) The expression of PGAM5, p-DRP1 (Ser 637), NRF2 and HO-1 were detected at indicated times after LFHP-1c treatment in rBMECs by immunoblotting, $n = 3$ per group. (B) and (C) IP/Western blotting results reveal that LFHP-1c treatment significantly reduced the interaction of PGAM5 with NRF2, $n = 3$ per group. (D) LFHP-1c facilitates nuclear translocation of NRF2 in rBMECs, $n = 3$ per group. (E) Silencing efficiency of siRNA against PGAM5 in rBMECs was verified by immunoblotting, $n = 3$ per group. (F) and (G) LFHP-1c treatment or knockdown of *Pgam5* facilitates nuclear translocation of NRF2 in rBMECs, and LFHP-1c treatment after si-PGAM5 did not affect the nuclear translocation of NRF2, $n = 3$ per

mRNA expression of *Ho-1* and *Nqo1* (Fig. 4K) in isolated rat cerebral microvessels after ischemic injury compared to vehicle group.

3.7. *LFHP-1c ameliorates brain ischemic injury in tMCAO model of M. fascicularis through PGAM5−NRF2 axis*

We further examined the effect of LFHP-1c against brain damage induced by transient middle cerebral artery occlusion in nonhuman primate *M. fascicularis* monkeys (Fig. 5A). The MRI data show that monkeys subjected to tMCAO resulted in brain infarct with a volume of 10.082 ± 2.848% of total brain at 3 days post-ischemia, and the infarct volume rate was decreased to 6.655 ± 1.478% by LFHP-1c administration (Fig. 5B and D). At 7 days after ischemia onset, the infarct volume rate was also attenuated in LFHP-1c group compared to vehicle-treated group (Fig. 5B and E, 13.762 ± 2.599% to 8.096 ± 2.937%). Moreover, the ratio of brain edema volume to total brain volume was decreased from 16.370 ± 5.527% to 5.084 ± 1.797% (Fig. 5C and F) and from 12.515 ± 3.017% to 6.140 ± 1.234% (Fig. 5C and G) by LFHP-1c administration at three or 7 days post-ischemia, respectively. Furthermore, LFHP-1c modestly improved neurological deficit induced by tMCAO injury at 1, 3, 5, 7 and 14 days post-ischemia (Fig. 5H and I). These results indicate that LFHP-1c tended to decrease brain infarct volume and brain edema and improve neurological deficits in *M. fascicularis* model with tMCAO.

The protein expressions of endothelial adhesion molecules (VCAM-1 and ICAM-1) and tight junction protein occludin in cerebral cortex of *M. fascicularis* after tMCAO injury were further investigated. VCAM-1 protein expression (Fig. 5J and K) and *VCAM*-1 mRNA expression (Fig. 5L) were significantly reduced by LFHP-1c treatment compared to vehicle group. LFHP-1c treatment decreased *ICAM*-1 mRNA expression and enhanced occludin mRNA expression (Fig. 5L). We further examined PGAM5−NRF2 axis after LFHP-1c treatment in cerebral cortex of *M. fascicularis*. LFHP-1c treatment decreased PGAM5 expression (Fig. 5J and K) and inhibited the phosphatase activity of PGAM5, indicated by the increase in expression of phosphorylation of DRP1 at Ser 637 site (Fig. 5J and K) compared to Vehicle group. Additionally, LFHP-1c treatment significantly enhanced NRF2 protein expression and stimulated HO-1 protein expression (Fig. 5J and K) compared to vehicle group. These results indicate that LFHP-1c treatment would ameliorate brain ischemic injury in tMCAO model of *M. fascicularis* through PGAM5−NRF2 axis.

4. Discussion

Ischemic stroke causes serious disability and mobility worldwide with limited effective therapeutics, thus it is urgent to develop novel drugs for the therapy of ischemic stroke[1]. In the present study, we demonstrated that LFHP-1c reduced brain infarct size and brain edema and improved neurological deficits in a rat model of tMCAO, with the therapeutic window expanded to 12 h. Further, we assessed the clinical translational potential of LFHP-1c with a tMCAO model in nonhuman primate *M. fascicularis*, a recognized pre-clinical evaluation model for cerebral ischemic stroke. Our results show that LFHP-1c could also attenuate infarct volume and brain edema and reduced the loss of neurological function in the *M. fascicularis* model of tMCAO, indicating LFHP-1c as a promising drug candidate for the treatment of ischemic stroke.

Abundant evidences support that BBB integrity maintains brain homeostasis, and BBB dysfunction occurs in the acute stage of ischemic stroke, leading to a serious brain edema and brain damage[3,32]. We showed that LFHP-1c improved TEER and reduced FITC-dextran permeability in *vitro* BBB model after OGD/R-injury, implying the BBB protection of LFHP-1c. Our data also show that LFHP-1c prevented the degradation of tight junction proteins ZO-1, occludin and claudin-5, and decreased the expression of endothelial adhesion molecules (*Vcam-1*, *Icam-1*), *Tnf-α*, *Mcp-1* and matrix metalloproteinases (*Mmp 2* and *Mmp 9*) in isolated rat brain microvessels at 3 days after tMCAO-injury. Furthermore, we observed that LFHP-1c treatment reduced VCAM-1 production and enhanced the expression of tight junction protein occludin in the peri-infarct region of *M. fascicularis* cortex. Various studies have showed that BBB protection is a benefit driver for neuroprotection and neurological recovery[33]. It is well-known that BBB mainly comprised brain microvascular endothelial cells, astrocytes, pericytes and basement membrane, and BBB is an active interface between the circulation and the central nervous system (CNS), maintaining the neural microenvironment with a dual function: the barrier function restricts transport of potentially toxic or harmful substances from the blood to the brain, and the carrier function is responsible for the transport of nutrients to the brain and removal of metabolites[34]. Our previous study demonstrated that LFHP-1c administration promoted the long-term sensorimotor functional recovery of rats over a period of 3 weeks after tMCAO[21]. Therefore, administration with LFHP-1c protects BBB integrity, so as to restore BBB functions and transport nutrients for the repair of damaged cells tissue. Our results indicate that LFHP-1c protects BBB integrity and ameliorate endothelial inflammation, which may contribute to the neuroprotection and neurological recovery of LFHP-1c.

Oxidative stress, leading to the imbalance between ROS production and impaired antioxidant system, is closely associated with endothelial dysfunction in various diseases[35], especially in ischemic stroke.[36,37]. Evidences demonstrate that oxidative stress occurs after cerebral ischemia and reperfusion and triggers brain ischemic damage[38]. It has been reported that microvascular endothelial cells are one of the main sources of ROS after cerebral ischemia−reperfusion[39]. Thus, preventing cerebral endothelial cells from oxidative stress may be a promising target to maintain BBB integrity and protect against BBB disruption after transient

group. (H) Fluorescence staining of NRF2 shows that LFHP-1c treatment or knockdown of *Pgam5* promoted NRF2 nuclear translocation, $n = 3$ per group. The scale bar represents 20 μm. (I) and (J) The protein expressions of PGAM5, p-DRP1 (Ser637), NRF2 and HO-1 in rat brain microvessels were detected at 72 h after tMCAO onsetand representative blots are shown here, $n = 4$ per group. (K) The mRNA expression of *Ho-1* and *Nqo1* was measured by RT-PCR, $n = 4−5$ per group. Results are expressed as mean ± SEM. For Fig. 4C, $^{***}P < 0.001$ *versus* IgG plus DMSO group, $^{\#\#}P < 0.01$ *versus* PGAM5 plus LFHP-1c (2 μmol/L) group. For Fig. 4D, $^{*}P < 0.05$, $^{***}P < 0.001$ *versus* '0' time point group. For Fig. 4E, $^{***}P < 0.001$ *versus* scramble group. For Fig. 4G, $^{***}P < 0.001$ *versus* scramble plus DMSO group. For Fig. 4J and K, $^{*}P < 0.05$, $^{**}P < 0.01$, $^{***}P < 0.001$ *versus* Sham group; $^{\#}P < 0.05$, $^{\#\#}P < 0.01$, $^{\#\#\#}P < 0.001$ *versus* Vehicle group.

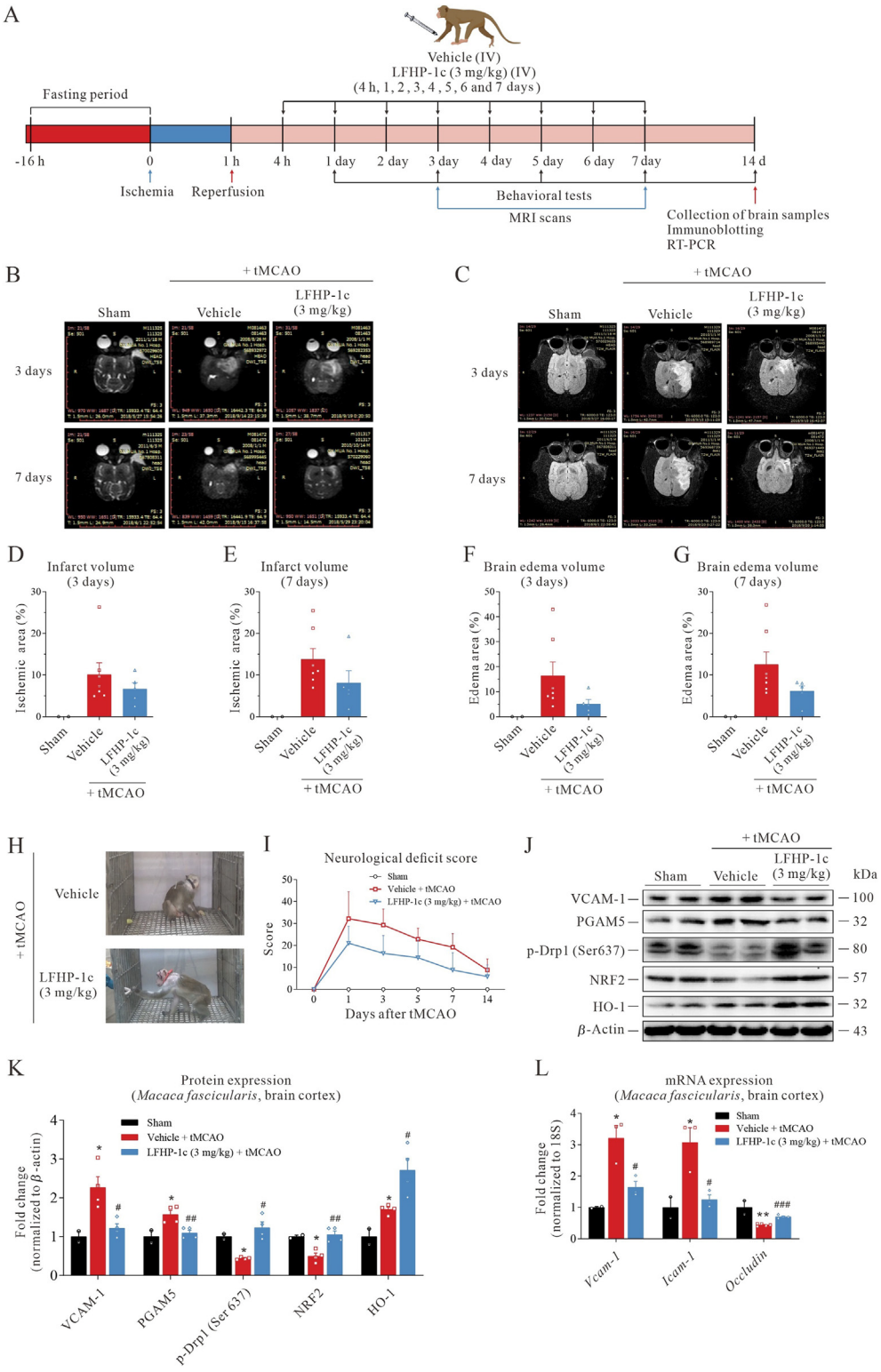

Figure 5 LFHP-1c ameliorates brain ischemic injury in tMCAO model of *Macaca fascicularis* through PGAM5−NRF2 pathway. (A) Experimental design of tMCAO to study the effects of LFHP-1c against ischemic stroke in *Macaca fascicularis*. (B)−(G) The brain infarct volume (B, D, and E) and edema volume (C, F, and G) were measured at three and 7 days after tMCAO onset by MRI, $n = 2-7$ per group. (H) and (I) Neurological deficit induced by tMCAO-injury was evaluated at 1, 3, 5, 7 and 14 days post-ischemia. (J) and (K) The protein expressions of VCAM-1, PGAM5, p-DRP1 (Ser 637), NRF2 and HO-1 in cerebral cortex of the brain of *Macaca fascicularis* were detected at 14 days after tMCAO onset, $n = 2-4$ per group. (L) The mRNA expression of *VCAM-1*, *ICAM-1* and occludin was measured by RT-PCR, $n = 2-4$ per group. Results are expressed as mean ± SEM. $^{*}P < 0.05$, $^{**}P < 0.01$ *versus* Sham group; $^{\#}P < 0.05$, $^{\#\#}P < 0.01$, $^{\#\#\#}P < 0.001$ *versus* Vehicle group.

ischemic injury. In our previous study, we demonstrated that LFHP-1c markedly increased NRF2 expression in primary microglia under normal condition and ischemia condition[21]. In this study, we show that LFHP-1c also significantly upregulated NRF2 expression and facilitated nuclear translocation of NRF2, and thus further stimulated the downstream genes *Ho-1* and *Nqo1* expression. Furthermore, we found that LFHP-1c reduced ROS production in rBMECs exposed to OGD/R injury, which was abolished by knockdown of NRF2 (Supporting Information Fig. S8). In addition, LFHP-1c treatment enhanced NRF2 accumulation and HO-1 expression in isolated rat brain microvessels and *M. fascicularis* cortex, which confirmed that NRF2 activation was involved in the effect of LFHP-1c on endothelial protection. These results implied that LFHP-1c amelioration of OGD/R-induced ROS accumulation may dependent on NRF2 activation.

PGAM5 is a mitochondrial Ser/Thr phosphatase normally located in the inner mitochondrial membrane[6,7] and plays an important role in regulating organelle homeostasis. But until now, there are no reports on small molecular inhibitors of PGAM5. It has been reported that PGAM5 could tether a ternary complex with KEAP1 and NRF2 to sequester NRF2 in the cytosol[16], and thereby prevents nuclear translocation of NRF2, following by repressing the transcription of NRF2-denpenent antioxidative genes[17,18]. However, there are fewer researches on the relationship between PGAM5—NRF2 interaction and ischemic stroke. In our study, we found a first small molecular compound LFHP-1c directly binding with PGAM5, could inhibit the PGAM5 phosphatase activity and interrupt the interaction between PGAM5 and NRF2, thus facilitate nuclear translocation of NRF2, and finally promote the production of downstream antioxidant genes and proteins such as HO-1 and NQO1, resulting in protection against BBB disruption and ischemic injury (Fig. 6).

LFHP-1c directly binding with PGAM5, not only interrupted the interaction between PGAM5 and NRF2, but also inhibited its enzyme activity and increased the expression of phosphorylation of DRP1 at Ser 637 site, which maybe promote mitochondrial fusion to provide energy for cell repair. In accordance with our previous studies reported in microglia[21], LFHP-1c may also regulate AMPK activity by phosphorylation in endothelial cells to produce ATP for cell repair. Also, the specific binding sites between LFHP-1c and PGAM5, and the mode of action between PGAM5 and NRF2 with LFHP-1c, need to be further determined. According to previous reports[16,17], we propose a hypothesis that PGAM5, KEAP1 and NRF2 bind with each other to form a stable complex as a triangle, and LFHP-1c may only interrupt the interaction between PGAM5 and NRF2 to destroy the stability of the ternary complex, which may result in decreased ubiquitination of NRF2 and facilitating nuclear translocation of NRF2, thereby promoting the transcription of NRF2-dependent antioxidative genes. However, the possible mode of action between LFHP-1c and the ternary complex needs to be further clarified by co-crystallization. Unfortunately, we have not got the co-crystal of PGAM5 and LFHP-1c or the ternary complex yet because of the complexity of the PGAM5 protein and the low water solubility of LFHP-1c. We are now transforming LFHP-1c into a salt form in order to increase its water solubility while optimizing the structure of LFHP-1c for the structure—activity relationship for better preclinical lead compounds for the therapy of ischemic stroke in the future. In this study, we found that LFHP-1c had no effects on the

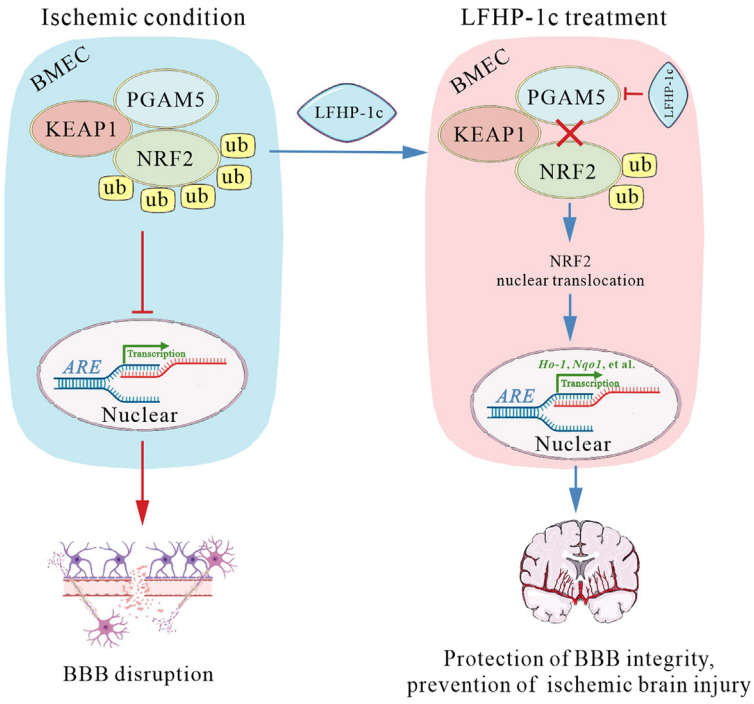

Figure 6 Schematic diagram of LFHP-1c protection on BBB disruption and ischemic brain injury. LFHP-1c is here reported as a novel PGAM5 inhibitor with beneficial effects on protection of brain microvascular endothelial cells (BMECs) and blood—brain barrier (BBB) integrity after stroke. By direct binding to PGAM5, LFHP-1c not only inhibits the PGAM5 enzyme activity, but also impairs the interaction between PGAM5 and NRF2, subsequently facilitates nuclear translocation of NRF2, thereby promotes the transcription activity of NRF2 to prevent endothelial injury, and finally protects against BBB disruption and ischemic brain injury.

expression of PGAM5 protein in endothelial cells, but attenuated the PGAM5 expression in the brain of rats after tMCAO. Until now, we have not fully elucidated the role of PGAM5 on the overall level of cerebral ischemia. Some studies showed that AMPK activation could inhibit the expression of PGAM5[40,41]. Previous studies in our group have shown that LFHP-1c inhibited microglia activation through activating AMPK/NRF2 pathway, and thus protecting cerebral ischemia[21]. The previous work was focused on anti-neuroinflammation and neuroprotection of LFHP-1c. After ischemic stroke, the neurons in the ischemic core would die within minutes of ischemia, followed by neuroinflammation mainly mediated by microglia/macrophages, subsequently the BBB damage[42]. Thus, we proposed that the intercellular interaction may affect the expression of PGAM5 in the brain, which might cause regulation of PGAM5 expression by LFHP-1c in the ischemic brain. In this study, we mainly focus on the BBB protection of LFHP-1c through interacting with PGAM5 in endothelia cells *in vitro* and *in vivo*. Our precious study has illustrated that LFHP-1c inhibited neuroinflammation *in vitro* and *in vivo*. It has reported that PGAM5 induces necroptosis and inflammation in microglia in encephalomyelitis (EAE) model[43] and promotes inflammasome activation in BMDM[44], suggesting that PGAM5 may also be the target for anti-neuroinflammation role of LFHP-1c in microglia. Therefore, we cannot rule out the beneficial effects of LFHP-1c on other cells to protect against cerebral ischemia *in vivo*. The brain microvascular endothelial cell-specific *Pgam5* knockout mice may clarify the LFHP-1c specific role in ischemic stroke. Pu et al.[45] have constructed a specific brain endothelial cell-specific Cre (BEC-Cre) mouse, but it needs more experiments to prove the usability of this kind of Cre mouse. This kind of mouse may be used to generate brain endothelial cell-specific *Pgam5* knockout mouse for our future study. When endothelial cells were exposed under OGD/R with tPA, LFHP-1c could not increase the tight junction protein occludin expression (data not shown), indicating that LFHP-1c may not have beneficial effects on tPA-caused endothelial injury, but it needs to be further investigated *in vivo* in the future. Also, besides PGAM5, LFHP-1c may also bind with other possible target proteins for BBB protection (Table S3), which need to be further validated to fully elucidate the beneficial effects of LFHP-1c *in vivo*.

5. Conclusions

In summary, LFHP-1c attenuated brain infarct and brain edema and improved neurological deficits induced by tMCAO in rats and non-human primates, and these effects may attribute to the protection of brain microvascular endothelial cells and BBB integrity by LFHP-1c through PGAM5−NRF2 axis. Therefore, LFHP-1c as a PGAM5 inhibitor would be a promising agent for BBB protection and a potential lead compound for the treatment of ischemic stroke, which is worth to be tested in clinic.

Acknowledgments

This work was supported by the National Natural Science Foundation of China (81973512, 81822041, 21977116, and 81673305), National Science & Technology Major Project "Key New Drug Creation and Manufacturing Program" (No. 2018ZX09711002-006-013, China), Science & Technology Major Project of Zhongshan City (No. 2019A4020, China), Double First-Class Project of China Pharmaceutical University (CPU2018GY06, CPU2018GY18, and CPU2018GY20, China), the Open Project of State Key Laboratory of Natural Medicines (SKLNMZZCX 201824 and SKLNMZZ202029, China), the Open Project Program of the State Key Laboratory of Drug Research (SIMM2004KF-08, China), the Open Project of Zhejiang Provincial Preponderant and Characteristic Subject of Key University (Traditional Chinese Pharmacology, China), Zhejiang Chinese Medical University (No. ZYAOX2018001, China), and State Key Laboratory of Pathogenesis, Prevention and Treatment of High Incidence Diseases in Central Asia Fund (SKL-HIDCA-2018-1, China). This work was also supported by the Six Talent Peaks Project of Jiangsu Province to Tao Pang. We sincerely thank websites BioRender and SMART for providing some of drawing materials. We appreciate technical support by the Public Experimental Pharmacology Platform of China Pharmaceutical University, Nanjing, China.

Author contributions

Chenglong Gao, Yazhou Xu, Zhuangzhuang Liang, Yunjie Wang, Qinghong Shang, and Shengbin Zhang performed the experiments of this work; Cunfang Wang, Mingmin Ni, Dalei Wu, Zhangjian Huang, and Tao Pang designed the research. Chenglong Gao, Yazhou Xu, and Zhuangzhuang Liang wrote the manuscript. Zhangjian Huang and Tao Pang supervised the project.

Conflicts of interest

Shengbin Zhang, Cunfang Wang and Mingmin Ni are full-time employees in Guangdong Long Fu Pharmaceutical Co., Ltd. (Zhongshan, China). All authors declare that they have no conflict of interest.

Appendix A. Supporting information

Supporting data to this article can be found online at https://doi.org/10.1016/j.apsb.2021.01.008.

References

1. Benjamin EJ, Blaha MJ, Chiuve SE, Cushman M, Das SR, Deo R, et al. Heart disease and stroke statistics-2017 update: a report from the American Heart Association. *Circulation* 2017;**135**:e146−603.
2. Tang J, Kang Y, Huang L, Wu L, Peng Y. TIMP1 preserves the blood−brain barrier through interacting with CD63/integrin 1 complex and regulating downstream FAK/RhoA signaling. *Acta Pharm Sin B* 2020;**10**:987−1003.
3. Borlongan CV, Rodrigues Jr AA, Oliveira MC. Breaking the barrier in stroke: what should we know? A mini-review. *Curr Pharm Des* 2012;**18**:3615−23.
4. Sandoval KE, Witt KA. Blood−brain barrier tight junction permeability and ischemic stroke. *Neurobiol Dis* 2008;**32**:200−19.
5. Shekhar S, Cunningham MW, Pabbidi MR, Wang S, Booz GW, Fan F. Targeting vascular inflammation in ischemic stroke: recent developments on novel immunomodulatory approaches. *Eur J Pharmacol* 2018;**833**:531−44.
6. Ruiz K, Thaker TM, Agnew C, Miller-Vedam L, Trenker R, Herrera C, et al. Functional role of PGAM5 multimeric assemblies and their polymerization into filaments. *Nat Commun* 2019;**10**:531.
7. Tipton P, Su T, Hannink M. Assembly of PGAM5 into multimeric complexes provides a mechanism for allosteric regulation of phosphatase activity. *Methods Enzymol* 2018;**607**:353−72.

8. Bernkopf DB, Jalal K, Brückner M, Knaup KX, Gentzel M, Schambony A, et al. PGAM5 released from damaged mitochondria induces mitochondrial biogenesis *via* Wnt signaling. *J Cell Biol* 2018;**217**:1383−94.
9. Rigden DJ. The histidine phosphatase superfamily: structure and function. *Biochem J* 2008;**409**:333−48.
10. Jedrzejas MJ. Structure, function, and evolution of phosphoglycerate mutases: comparison with fructose-2,6-bisphosphatase, acid phosphatase, and alkaline phosphatase. *Prog Biophys Mol Biol* 2000;**73**:263−87.
11. Panda S, Srivastava S, Li Z, Vaeth M, Fuhs SR, Hunter T, et al. Identification of PGAM5 as a mammalian protein histidine phosphatase that plays a central role to negatively regulate $CD4^+$ T cells. *Mol Cell* 2016;**63**:457−69.
12. Takeda K, Komuro Y, Hayakawa T, Oguchi H, Ishida Y, Murakami S, et al. Mitochondrial phosphoglycerate mutase 5 uses alternate catalytic activity as a protein serine/threonine phosphatase to activate ASK1. *Proc Natl Acad Sci U S A* 2009;**106**:12301−5.
13. Park YS, Choi SE, Koh HC. PGAM5 regulates PINK1/PARKIN-mediated mitophagy *via* DRP1 in CCCP-induced mitochondrial dysfunction. *Toxicol Lett* 2018;**284**:120−8.
14. Liu L, Feng D, Chen G, Chen M, Zheng Q, Song P, et al. Mitochondrial outer-membrane protein FUNDC1 mediates hypoxia-induced mitophagy in mammalian cells. *Nat Cell Biol* 2012;**14**:177−85.
15. Lu W, Karuppagounder SS, Springer DA, Allen MD, Zheng L, Chao B, et al. Genetic deficiency of the mitochondrial protein PGAM5 causes a Parkinson's-like movement disorder. *Nat Commun* 2014;**5**:4930.
16. Lo SC, Hannink M. PGAM5 tethers a ternary complex containing KEAP1 and NRF2 to mitochondria. *Exp Cell Res* 2008;**314**:1789−803.
17. Hos NJ, Ganesan R, Gutiérrez S, Hos D, Klimek J, Abdullah Z, et al. Type I interferon enhances necroptosis of typhimurium-infected macrophages by impairing antioxidative stress responses. *J Cell Biol* 2017;**216**:4107−21.
18. Robinson N. Typhimurium infection: type I interferons integrate cellular networks to disintegrate macrophages. *Cell Stress* 2018;**2**:37−9.
19. Chen Y, Gong K, Xu Q, Meng J, Long T, Chang C, et al. Phosphoglycerate mutase 5 knockdown alleviates neuronal injury after traumatic brain injury through DRP1-mediated mitochondrial dysfunction. *Antioxid Redox Signal* 2021;**34**:154−70.
20. Yang T, Sun Y, Mao L, Zhang M, Li Q, Zhang L, et al. Brain ischemic preconditioning protects against ischemic injury and preserves the blood−brain barrier *via* oxidative signaling and NRF2 activation. *Redox Biol* 2018;**17**:323−37.
21. Wang Y, Huang Y, Xu Y, Ruan W, Wang H, Zhang Y, et al. A dual AMPK/NRF2 activator reduces brain inflammation after stroke by enhancing microglia M2 polarization. *Antioxid Redox Signal* 2018;**28**:141−63.
22. Sasaki M, Honmou O, Radtke C, Kocsis JD. Development of a middle cerebral artery occlusion model in the nonhuman primate and a safety study of i.v. infusion of human mesenchymal stem cells. *PLoS One* 2011;**6**:e26577.
23. Wang H, Xu X, Guan X, Shen S, Huang X, Kai G, et al. Liposomal 9-aminoacridine for treatment of ischemic stroke: from drug discovery to drug delivery. *Nano lett* 2020;**20**:1542−51.
24. Wang J, Li C, Chen T, Fang Y, Shi X, Pang T, et al. Nafamostat mesilate protects against acute cerebral ischemia *via* blood−brain barrier protection. *Neuropharmacology* 2016;**105**:398−410.
25. Kito G, Nishimura A, Susumu T, Nagata R, Kuge Y, Yokota C, et al. Experimental thromboembolic stroke in cynomolgus monkey. *J Neurosci Methods* 2001;**105**:45−53.
26. Feng H, Hu L, Zhu H, Tao L, Wu L, Zhao Q, et al. Repurposing antimycotic ciclopirox olamine as a promising anti-ischemic stroke agent. *Acta Pharm Sin B* 2020;**10**:434−46.
27. Gao CL, Hou GG, Liu J, Ru T, Xu YZ, Zhao SY, et al. Synthesis and target identification of benzoxepane derivatives as potential anti-neuroinflammatory agents for ischemic stroke. *Angew Chem Int Ed Engl* 2020;**59**:2429−39.
28. Nakagawa S, Deli MA, Kawaguchi H, Shimizudani T, Shimono T, Kittel A, et al. A new blood−brain barrier model using primary rat brain endothelial cells, pericytes and astrocytes. *Neurochem Int* 2009;**54**:253−63.
29. Dejana E. Endothelial cell−cell junctions: happy together. *Nat Rev Mol Cell Biol* 2004;**5**:261−70.
30. Mackinnon AL, Taunton J. Target identification by diazirine photo-cross-linking and click chemistry. *Curr Protoc Chem Biol* 2009;**1**:55−73.
31. Zhu D, Guo H, Chang Y, Ni Y, Li L, Zhang ZM, et al. Cell- and tissue-based proteome profiling and dual imaging of apoptosis markers with probes derived from venetoclax and idasanutlin. *Angew Chem Int Ed Engl* 2018;**57**:9284−9.
32. Engelhardt B, Liebner S. Novel insights into the development and maintenance of the blood−brain barrier. *Cell Tissue Res* 2014;**355**:687−99.
33. Xue Q, Liu Y, He R, Yang S, Tong J, Li X, et al. Lyophilized powder of catalpol and puerarin protects neurovascular unit from stroke. *Int J Biol Sci* 2016;**12**:367−80.
34. Lv J, Hu W, Yang Z, Li T, Jiang S, Ma Z, et al. Focusing on Claudin-5: a promising candidate in the regulation of BBB to treat ischemic stroke. *Prog Neurobiol* 2018;**161**:79−96.
35. Santilli F, D'Ardes D, Davi G. Oxidative stress in chronic vascular disease: from prediction to prevention. *Vasc Pharmacol* 2015;**74**:23−37.
36. Yang Q, Huang Q, Hu Z, Tang X. Potential neuroprotective treatment of stroke: targeting excitotoxicity, oxidative stress, and inflammation. *Front Neurosci* 2019;**13**:1036.
37. Wang J, Huang L, Cheng C, Li G, Xie J, Shen M, et al. Design, synthesis and biological evaluation of chalcone analogues with novel dual antioxidant mechanisms as potential anti-ischemic stroke agents. *Acta Pharm Sin B* 2019;**9**:335−50.
38. Mehta SL, Manhas N, Raghubir R. Molecular targets in cerebral ischemia for developing novel therapeutics. *Brain Res Rev* 2007;**54**:34−66.
39. Kontos CD, Wei EP, Williams JI, Kontos HA, Povlishock JT. Cytochemical detection of superoxide in cerebral inflammation and ischemia *in vivo*. *Am J Physiol* 1992;**263**:H1234−42.
40. Wang YS, Yu P, Wang Y, Zhang J, Hang W, Yin ZX, et al. AMP-activated protein kinase protects against necroptosis *via* regulation of KEAP1−PGAM5 complex. *Int J Cardiol* 2018;**259**:153−62.
41. Liu X, Xu C, Xu L, Li X, Sun H, Xue M, et al. Empagliflozin improves diabetic renal tubular injury by alleviating mitochondrial fission *via* AMPK/SP1/PGAM5 pathway. *Metabolism* 2020;**111**:154334.
42. Zhou Z, Lu J, Liu WW, Manaenko A, Hou X, Mei Q, et al. Advances in stroke pharmacology. *Pharmacol Ther* 2018;**191**:23−42.
43. Wang Y, Bi Y, Xia Z, Shi W, Li B, Li B, et al. Butylphthalide ameliorates experimental autoimmune encephalomyelitis by suppressing PGAM5-induced necroptosis and inflammation in microglia. *Biochem Biophys Res Commun* 2018;**497**:80−6.
44. Moriwaki K, Farias Luz N, Balaji S, de Rosa MJ, O'Donnell CL, Gough PJ, et al. The mitochondrial phosphatase PGAM5 is dispensable for necroptosis but promotes inflammasome activation in macrophages. *J Immunol* 2016;**196**:407−15.
45. Pu W, He L, Han X, Tian X, Li Y, Zhang H, et al. Genetic targeting of organ-specific blood vessels. *Circ Res* 2018;**123**:86−99.